Article

Cell Metabolism

Zfp423 Maintains White Adipocyte Identity through Suppression of the Beige Cell Thermogenic Gene Program

Graphical Abstract

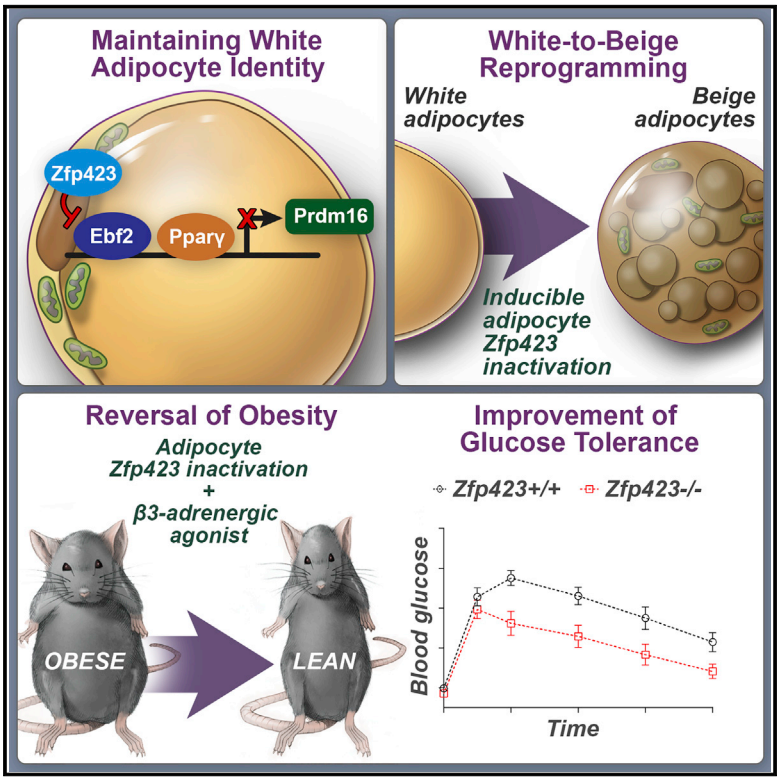

Authors

Mengle Shao, Jeff Ishibashi, Christine M. Kusminski, ..., William L. Holland, Patrick Seale, Rana K. Gupta

Correspondence

rana.gupta@utsouthwestern.edu

In Brief

How white adipocytes suppress their thermogenic gene program has remained unclear. Here, Shao et al. identify Zfp423 as a molecular brake on adipocyte thermogenesis through inhibition of Ebf2 activity. Inducible deletion of *Zfp423* in obese mice triggers white-to-beige adipocyte reprogramming and reversal of obesity and insulin resistance.

Highlights

- Deletion of adipocyte *Zfp423* triggers a white-to-beige fat cell conversion
- Converted beige fat cells, when activated, reverse diet-induced obesity
- Zfp423 inhibits the adipocyte thermogenic gene program through repression of Ebf2
- The Zfp423-Ebf2 protein complex is inhibited by BMP7-Smad signaling

Accession Numbers

GSE74899

Shao et al., 2016, Cell Metabolism *23*, 1167–1184
June 14, 2016
http://dx.doi.org/10.1016/j.cmet.2016.04.023

Cell Metabolism
Article

Zfp423 Maintains White Adipocyte Identity through Suppression of the Beige Cell Thermogenic Gene Program

Mengle Shao,[1] Jeff Ishibashi,[2] Christine M. Kusminski,[1] Qiong A. Wang,[1] Chelsea Hepler,[1] Lavanya Vishvanath,[1] Karen A. MacPherson,[1] Stephen B. Spurgin,[1] Kai Sun,[1] William L. Holland,[1] Patrick Seale,[2] and Rana K. Gupta[1,*]
[1]Touchstone Diabetes Center and Department of Internal Medicine, University of Texas Southwestern Medical Center, Dallas, TX 75390, USA
[2]Institute for Diabetes, Obesity and Metabolism and Department of Cell and Developmental Biology, Perelman School of Medicine, University of Pennsylvania, Philadelphia, PA 19104, USA
*Correspondence: rana.gupta@utsouthwestern.edu
http://dx.doi.org/10.1016/j.cmet.2016.04.023

SUMMARY

The transcriptional regulators Ebf2 and Prdm16 establish and maintain the brown and/or beige fat cell identity. However, the mechanisms operating in white adipocytes to suppress the thermogenic gene program and maintain an energy-storing phenotype are less understood. Here, we report that the transcriptional regulator Zfp423 is critical for maintaining white adipocyte identity through suppression of the thermogenic gene program. Zfp423 expression is enriched in white versus brown adipocytes and suppressed upon cold exposure. Doxycycline-inducible inactivation of *Zfp423* in mature adipocytes, combined with β-adrenergic stimulation, triggers a conversion of differentiated *adiponectin*-expressing inguinal and gonadal adipocytes into beige-like adipocytes; this reprogramming event is sufficient to prevent and reverse diet-induced obesity and insulin resistance. Mechanistically, Zfp423 acts in adipocytes to inhibit the activity of Ebf2 and suppress *Prdm16* activation. These data identify Zfp423 as a molecular brake on adipocyte thermogenesis and suggest a therapeutic strategy to unlock the thermogenic potential of white adipocytes in obesity.

INTRODUCTION

Adipocytes regulate several aspects of energy homeostasis in mammalian systems. White fat cells represent the main site of energy storage, containing a single, large lipid droplet and the enzymatic machinery to both synthesize and hydrolyze triglycerides. In addition, fat cells secrete numerous proteins that affect various aspects of energy homeostasis, including food intake, insulin sensitivity, and cardiovascular performance (Rosen and Spiegelman, 2014). In the setting of obesity, white adipose tissue (WAT) expands considerably to meet the increased demand for energy storage; however, this expansion can be pathological and can contribute directly to systemic metabolic dysfunction (Sun et al., 2011).

Most mammals contain a second class of adipocytes that function in adaptive thermogenesis (Cohen and Spiegelman, 2015). At least two subtypes of thermogenic adipocytes exist: brown and beige fat cells. Brown and beige fat cells are specialized to dissipate chemical energy in the form of heat and likely evolved to protect mammals from hypothermia (Cannon and Nedergaard, 2004). This thermogenic function is mediated predominantly by the presence of Ucp1, a protein that catalyzes a proton leak across the inner mitochondrial membrane. Brown adipocytes are organized into distinct depots and originate developmentally from a Myf5+ lineage (Seale et al., 2008). Beige fat cells exist as clusters found embedded within WAT depots, but most of these cells are not derived from a Myf5 lineage (Sanchez-Gurmaches and Guertin, 2014; Sanchez-Gurmaches et al., 2016); a number of studies suggest a smooth muscle-like origin for at least a subset of these cells (Long et al., 2014; McDonald et al., 2015). There is considerable interest and excitement over the possibility of stimulating the formation and activity of beige and brown adipocytes in humans as a therapeutic treatment for obesity and metabolic disease (Betz and Enerbäck, 2015; Schrauwen et al., 2015). Adult humans have existing beige and brown adipocytes, and these cells can be activated under a number of physiological or pharmacological conditions (Cypess et al., 2015; Lidell et al., 2013; Virtanen et al., 2009). However, it remains unclear whether there are sufficient numbers of thermogenic adipocytes present, particularly in obese individuals, to exert a long-term therapeutic effect (Cypess et al., 2015). Thus, considerable effort is being placed on elucidating the mechanisms controlling the formation of beige adipocytes from adipose precursors (adipogenesis) or other sources, with the hope of stimulating the recruitment of additional beige fat cells in obesity.

The establishment and maintenance of functional adipocytes are dependent on three critical events: (1) preadipose cell determination, involving the commitment of multipotent progenitors to the adipocyte lineage; (2) adipocyte differentiation, in which committed preadipose cells undergo a morphological and biochemical transition into mature adipocytes in response to appropriate cues; and (3) adipocyte maintenance, in which the cellular identity and functional properties of the terminally differentiated cells are maintained. The seminal breakthrough discovery in the field of adipogenesis was the identification of the

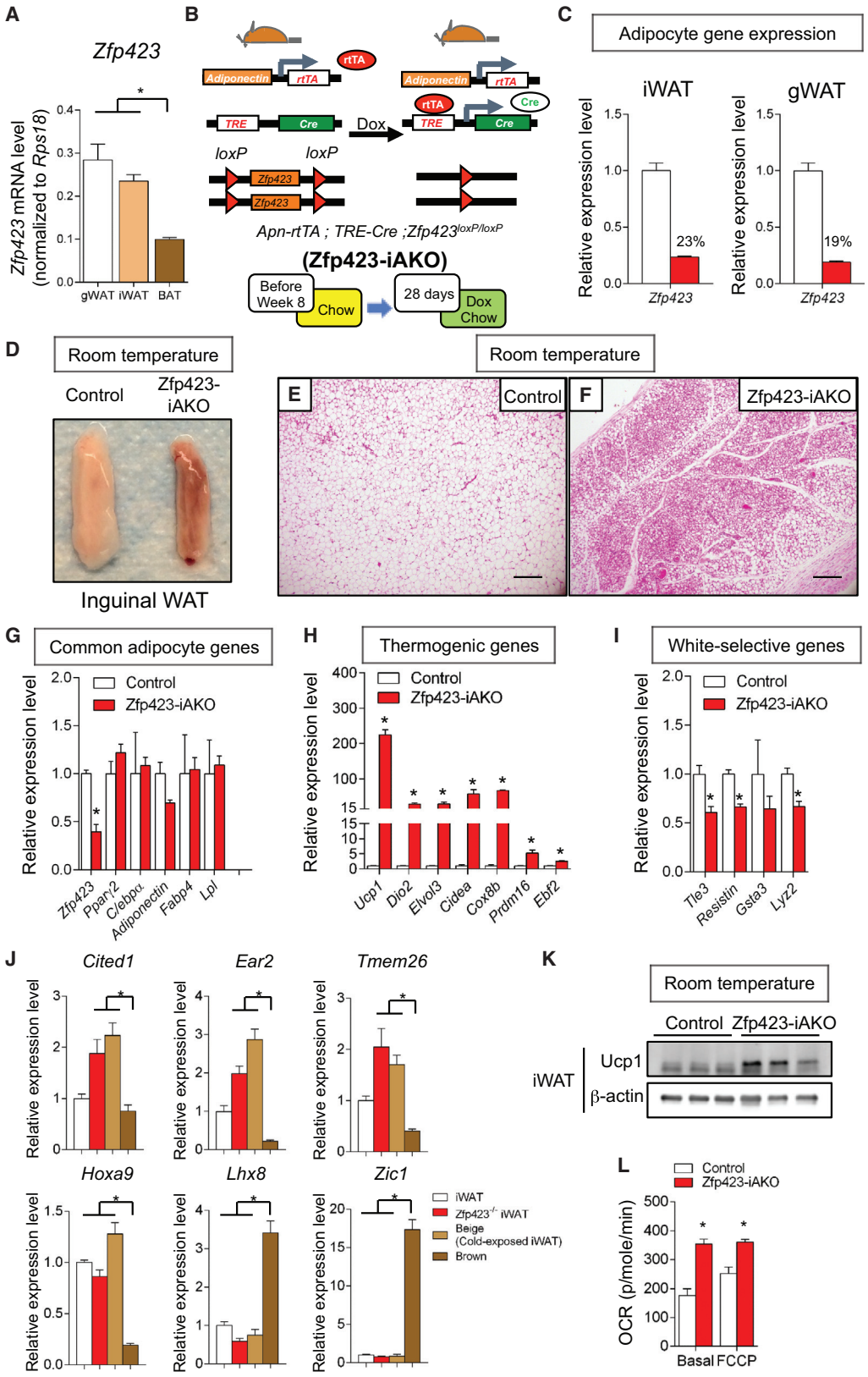

(legend on next page)

nuclear hormone receptor Pparγ as a differentiation-induced "master regulator" of adipocyte differentiation (Chawla et al., 1994; Tontonoz et al., 1994). The discovery of Pparγ left open the question of how the fates of specific subtypes of adipocytes were determined and maintained. Efforts to address this question led first to the discovery of Pgc-1α, a cold-induced co-activator of Pparγ whose function is to activate the thermogenic gene program (Puigserver et al., 1998). Since then, many other transcriptional regulators of thermogenesis and Pgc-1α activity have been identified (Kong et al., 2014; Seale, 2015). Another important breakthrough came with the discoveries of Prdm16, its co-regulator EHMT1, and the transcription factor Ebf2, all of which specify the brown and/or beige lineage from mesenchymal precursors (Ohno et al., 2013; Rajakumari et al., 2013; Seale et al., 2007). Ebf2 expression defines adipocyte precursors as brown or beige and coordinates with Pparγ to directly regulate the expression of *Prdm16* (Wang et al., 2014). The loss of Ebf2 in mice profoundly affects brown and beige adipocyte formation. Prdm16 and Ebf2 represent brown fat determination factors that establish and maintain the brown or beige adipocyte cellular identity; however, considerably less is known about the transcriptional components maintaining the identity and fate of white adipocytes. In particular, it remains unclear how mature white fat cells can resist activation of the thermogenic gene program, despite expressing many of same core transcriptional components. Moreover, whether this program can be sufficiently unlocked in white adipocytes of obese animals to help facilitate weight loss remains unknown.

We previously identified the C2H2 zinc-finger (ZF) protein, Zfp423, as a transcriptional regulator of preadipocyte determination (Gupta et al., 2010). Zfp423, functioning partly through co-activation of Smad proteins in the bone morphogenic protein (BMP) signaling cascade, regulates preadipocyte levels of *Pparγ* and adipogenesis. *Zfp423* expression defines committed preadipocyte mural cells that reside in the vasculature of adult adipose tissues (Gupta et al., 2012; Vishvanath et al., 2016). However, its expression persists throughout adipocyte differentiation and is present in all mature fat cells. Zfp423 regulates the formation of adipocytes; however, the function of Zfp423 in maintaining mature adipocyte function is unclear.

Here, we use a model for doxycycline (DOX)-inducible deletion of *Zfp423* in mature adipocytes of adult mice to reveal that Zfp423 suppresses the thermogenic gene program in fully differentiated white adipocytes. This occurs, at least partly, through direct repression of Ebf2 activity. Inducible genetic ablation of *Zfp423* in white adipocytes of adult animals leads to a conversion of mature white adipocytes into functional beige adipocytes, facilitating prevention and reversal of diet-induced obesity and impaired glucose homeostasis. Furthermore, we find that the transcriptional complex involving Zfp423 and Ebf2 is regulated by the brown fat determination factor BMP7, providing mechanistic insight into how BMP7 can promote brown adipogenesis and thermogenesis. Together, these data implicate Zfp423 as a white adipocyte determination factor, uncover a novel mechanism by which white adipocytes suppress their thermogenic gene program, and suggest a therapeutic strategy to unlock the thermogenic potential of white fat cells as a treatment for obesity and type 2 diabetes.

RESULTS

Adipocyte-Specific Inactivation of *Zfp423* Induced in Adult Mice Leads to Accumulation of Beige-like Adipocytes in WAT Depots

Our previous work revealed that *Zfp423* expression identifies preadipocytes (Gupta et al., 2010; Vishvanath et al., 2016). In this context, *Zfp423* regulates *Pparγ* expression and the potential of cells to undergo adipocyte differentiation. *Zfp423* expression persists throughout adipocyte differentiation, and *Zfp423* mRNA levels can be readily detected in purified adipocyte fractions obtained from gonadal white adipose tissue (gWAT), inguinal white adipose tissue (iWAT), and interscapular brown adipose tissue (BAT) depots of adult mice (Figure 1A). However, the abundance of *Zfp423* mRNA is significantly higher in white adipocytes compared to brown adipocytes (gWAT and iWAT versus BAT) (Figure 1A). Differential expression of Zfp423 in mature white versus brown adipocytes raises the possibility that this factor may play a role in controlling the functional properties of white or brown fat cells.

To investigate the function of *Zfp423* in fully differentiated mature adipocytes, we generated a novel mouse model in which *Zfp423* can be inactivated in *adiponectin*-expressing adipocytes in a DOX-dependent manner. The model consists of one transgene that expresses the reverse tetracycline transactivator (rtTA) under the control of a 5.4 kb promoter fragment of the

Figure 1. Widespread Accumulation of Beige-like Adipocytes in WAT Depots of Inducible Adipocyte-Specific *Zfp423* Knockout Mice

(A) mRNA levels of *Zfp423* in fractionated adipocytes isolated from anatomically distinct fat pads of adult C57BL/6 mice. One-way ANOVA, *p < 0.05, n = 6.

(B) Inducible inactivation of *Zfp423* in mature adipocytes (Zfp423-iAKO mice) is achieved by breeding the *Adiponectin*^{rtTA} transgenic mice to animals expressing Cre recombinase under the control of *TRE-Cre* and carrying floxed *Zfp423* alleles (*Zfp423*$^{loxP/loxP}$). Littermates carrying only *Adiponectin*^{rtTA} and *Zfp423*$^{loxP/loxP}$ alleles (i.e., Cre−) were used as control animals. Mice were kept at room temperature and fed normal chow until 8 weeks of age before being switched to a DOX-containing chow diet for another 28 days.

(C) Relative mRNA levels of *Zfp423* in fractionated adipocytes isolated from iWAT and gWAT of control (white bar) and Zfp423-iAKO (red bar) mice after DOX feeding. n = 4.

(D) Representative photograph of iWAT from control and Zfp423-iAKO mice after DOX feeding.

(E and F) Representative H&E staining of the iWAT section obtained from (E) a control mouse and (F) a Zfp423-iAKO mouse after DOX feeding. Scale bar, 200 μM.

(G–I) Relative mRNA levels of (G) common adipocyte genes, (H) brown- and/or beige-selective thermogenic genes, and (I) white adipocyte-selective genes in iWAT of control and Zfp423-iAKO mice after DOX feeding. Student's t test, *p < 0.05, n = 4.

(J) Relative mRNA levels of brown adipocyte- and beige adipocyte-selective markers in the iWAT depots of control mice (iWAT), Zfp423-iAKO mice (Zfp423$^{-/-}$ iWAT), cold-exposed control mice (beige), and BAT of control mice (brown) after DOX feeding. One-way ANOVA, *p < 0.05, n = 4–6.

(K) Western blot of Ucp1 protein levels in iWAT of control and Zfp423-iAKO mice after DOX feeding.

(L) Basal and maximal (FCCP) oxygen consumption rate (OCR) of diced iWAT isolated from control and Zfp423-iAKO mice after DOX feeding. Student's t test, *p < 0.05, n = 5.

adiponectin locus, another transgene in which Cre recombinase is expressed from a promoter containing the Tet-response element (TRE-Cre), and two conditional (loxP-flanked) *Zfp423* alleles (*Adiponectin^{rtTA}; TRE-Cre; Zfp423$^{loxP/loxP}$* animals, herein denoted as Zfp423-iAKO mice) (Figure 1B). In this system, the administration of DOX-containing chow diet to adult mice triggers Cre-mediated recombination specifically in terminally differentiated adipocytes (Wang et al., 2013). Accordingly, *Zfp423* mRNA levels are reduced by ~80% in the purified adipocyte fraction from both iWAT and gWAT of Zfp423-iAKO mice following the administration of a DOX-containing chow diet for 7 days (Figure 1C). Therefore, this system allows for the assessment of *Zfp423* function in both major white adipose depots.

We administered control (*Adiponectin^{rtTA}; TRE-Cre* mice or *Adiponectin^{rtTA}; Zfp423$^{loxP/loxP}$* animals) and Zfp423-iAKO mice DOX-containing chow diet at room temperature for 4 weeks, beginning at 8 weeks of age. After the 4-week period, a dramatic morphological change of WAT was observed in the Zfp423-iAKO mice. In particular, the iWAT depot of Zfp423-iAKO mice exhibited a uniform brown appearance (Figure 1D). H&E staining of iWAT sections revealed a widespread accumulation of multilocular, brown- and/or beige-like adipocytes in the *Zfp423*-deficient fat depot (Figures 1E and 1F). The mRNA levels of pan-adipocyte markers such as *Pparγ*, *C/ebpa*, *adiponectin*, *Fabp4*, and *Lpl* were not altered in *Zfp423*-deficient fat depots (Figure 1G); this suggests that Zfp423 is not required in mature adipocytes to maintain a fat cell identity per se. However, mRNA levels of key components of the adipocyte thermogenic gene program were robustly enriched in *Zfp423*-deficient WAT (Figure 1H), while mRNA levels of white adipocyte-selective genes were significantly downregulated (Figure 1I). Moreover, mRNA levels of genes described as beige selective were enriched in iWAT of Zfp423-iAKO mice; classic brown adipocyte markers remained low (Figure 1J) (Sharp et al., 2012; Shinoda et al., 2015). Most notably, levels of *Ucp1* mRNA were ~200-fold higher than those observed in tissues of control mice. Accordingly, protein levels of Ucp1 were enriched in the knockout tissue lysates and observed ubiquitously across histological sections (Figure 1K; Figure S1A). *Zfp423*-deficient WAT also appears to be more metabolically active. Both basal and maximum rates of oxygen consumption were significantly elevated in diced iWAT from the Zfp423-iAKO animals when compared to controls (Figure 1L).

The morphology and metabolic activity of iWAT from Zfp423-iAKO mice maintained at room temperature closely resembled beige adipocytes active in cold-exposed mice. To explore this more globally, we obtained and compared global microarray gene expression profiles of iWAT from control animals maintained at room temperature, control animals exposed to the cold for 14 days, and Zfp423-iAKO mice maintained at room temperature. In Zfp423-deficient iWAT, 270 transcripts were differentially regulated (±2-fold) when compared to iWAT from control animals maintained at room temperature (Table S1). Of these 270 transcripts, 140 (52%) were genes whose expression is regulated by cold exposure (Figure S2A). Functional classification of these 140 genes by gene ontology analysis indicated that nearly all of these genes are related to mitochondrial function and biogenesis, a hallmark of thermogenic adipocytes (Figure S2B).

Activation of the thermogenic gene program in WAT of the Zfp423-iAKO mice was not limited to the iWAT depot. Four weeks after the deletion of Zfp423, an induction in expression of genes of the thermogenic program was also observed in gWAT, albeit to a lesser degree (Figure S1B). However, expression of these same genes in interscapular BAT of Zfp423-iAKO mice was not significantly different from that observed in control animals (Figure S1C). This may be a result of the recombination efficiency in this depot. For reasons currently unclear, the *adiponectin*-driven rtTA transgene is not active in all interscapular brown adipocytes (Wang et al., 2013). Accordingly, we consistently observe <50% reduction in mRNA levels of *Zfp423* in this depot.

We also examined adipose depots of Zfp423-iAKO mice maintained on a DOX-containing chow diet for 16 weeks. In these animals, a significant morphological and molecular browning of all major WAT depots could be observed, including iWAT, peri-renal WAT, and gWAT (Figure S3). These data suggest that Zfp423 deletion can unlock the thermogenic gene program in white adipocytes but that an additional signal is needed to fully activate the thermogenic function of the cells.

It is well known that anatomically distinct depots differ in their thermogenic capacity. This is partly because of intrinsic differences in the distinct adipocytes. However, this is likely also because of differences in sympathetic innervation (activation of β3-adrenergic signaling) or immune response, both of which can modulate browning. We tested whether the additional signal needed to fully trigger browning of gWAT in Zfp423-iAKO mice was related to sympathetic outflow. In this experiment, we held animals at thermoneutrality while treating with DOX for 1 week to delete *Zfp423* (Figure S4). Inactivation of adipocyte *Zfp423* at thermoneutrality led to an increase in expression of Ucp1 and other genes of the thermogenic program; however, the effects were less robust than those observed in the aforementioned experiments performed at room temperature, and morphological changes adipose depots were not observed (Figure S4). We then treated mice at thermoneutrality with the β3-agonist CL316243 once daily for 3 days. Following treatment with the β3-receptor agonist, we observed a greater accumulation of beige adipocytes in iWAT of Zfp423-iAKO mice when compared to tissues from treated controls. Compared to the iWAT depot, the gWAT depot is normally quite resistant to the effects of pharmacological β3-receptor stimulation; however, deletion of *Zfp423* in gonadal adipocytes renders the depot capable of adopting a robust beige phenotype within 3 days of treatment, similar to that observed in normal iWAT depots. (Figure S4).

Beige-like Adipocytes in Zfp423-iAKO Mice Arise through Conversion of *adiponectin*-Expressing *Zfp423*-Deficient Adipocytes

White adipocytes in the iWAT depot of adult mice maintained on a standard chow diet at room temperature exhibit little turnover (Wang et al., 2013). However, beige adipocytes accumulate rapidly within the white adipose depots of mice exposed to cold temperatures. Lineage-tracing studies suggest that beige adipocytes can arise through a number of mechanisms. Studies have indicated that beige adipocytes likely arise largely through de novo differentiation from beige preadipocytes during the

period of cold exposure (Berry et al., 2016; Long et al., 2014; Vishvanath et al., 2016; Wang et al., 2013). Mature unilocular adipocytes can also adopt a beige adipocyte phenotype upon cold exposure. The specific unilocular adipocytes that become Ucp1+ multilocular cells may represent existing dormant beige adipocytes or bona fide white adipocytes undergoing a lineage conversion (for review, see Kajimura et al., 2015). The latter mechanisms are difficult to distinguish from one another due to a lack of suitable molecular markers.

We sought to determine the source of the beige adipocytes accumulating in the Zfp423-iAKO mice. In principle, the accumulated beige-like adipocytes could emerge through a conversion or reprogramming of Zfp423-deficient *adiponectin*$^{+}$ adipocytes. Alternatively, beige adipocytes can emerge from precursors in response to events triggered by *Zfp423* deletion in mature adipocytes. We employed pulse-chase lineage tracing to determine whether the beige adipocytes in the Zfp423-iAKO mice arise through direct conversion of existing *Zfp423*-deficient *adiponectin*$^{+}$ white adipocytes. We reconstituted the Cre-dependent *Rosa26R*$^{mT/mG}$ reporter to the Zfp423-iAKO animal background (Zfp423-iAKO; *Rosa26R*$^{mT/mG}$ animals) (Figure 2A). This allows for DOX-dependent inactivation of the *Zfp423* locus with simultaneous indelible membrane-bound GFP (mGFP) labeling of the targeted adipocytes. We administered DOX for 7 days at room temperature to ensure complete labeling and deletion of *Zfp423* (pulse). After this initial pulse-labeling period, Cre expression and the subsequent loss of *Zfp423* expression occur efficiently and specifically in the mature adipocyte fraction of the inguinal adipose depot (Figures 2B and 2C). Indirect immunofluorescence assays with anti-GFP antibodies indicated that nearly all adipocytes were expressed mGFP; however, at this time, no multilocular cells were present in control or knockout mice (Figures 2D–2F). Animals were then maintained at room temperature for 3 weeks in the absence of DOX (chase). After the 3-week period, large regions of multilocular cells were present only in the Zfp423-iAKO mice (Figures 2G–2I). All of the cells we observed continued to express mGFP (Figure 2H). This indicates that the beige adipocytes accumulating this model were derived from *Zfp423*-deficient *adiponectin*$^{+}$ adipocytes. As a control experiment, we also placed a cohort of control mice (*Adiponectin*^{rtTA}*; TRE-Cre; Rosa26R*$^{mT/mG}$ animals) at 6°C for 7 days after the pulse-labeling period. As expected and previously reported, both mGFP^{+} and mGFP^{-} cells were observed (Figure 2J), highlighting the ability of the model to capture the dual mechanisms used to recruit beige adipocytes upon cold exposure.

Finally, we asked whether the white-to-beige adipocyte conversion is observed in vitro in an adipocyte-autonomous manner. We isolated the stromal vascular fraction (SVF) of iWAT from control and Zfp423-iAKO animals and induced adipocyte differentiation in vitro for 10 days. We then treated fully differentiated cultures with DOX for 12 hr to inactivate *Zfp423* in adipocytes. Within 48 hr after the removal of DOX from differentiated cultures, we observed robust enrichment of mRNAs encoding key thermogenic genes in *Zfp423*-deficient adipocytes, including an ~15-fold induction of *UCP1* and an ~20-fold increase in *Dio2* (Figure 2K). These data indicate that *Zfp423*-deficient adipocytes can convert into Ucp1+ beige cells in a cell-autonomous manner. Zfp423 appears to be critical for the maintenance of white adipocyte cellular identity, and the loss of Zfp423 triggers a conversion of white adipocytes into beige fat cells.

Mice Lacking Adipocyte Zfp423 Are Resistant to Diet-Induced Obesity

A preponderance of evidence in the literature supports the notion that beige adipocytes can exert beneficial effects on glucose homeostasis and increase energy expenditure. Thus, we asked whether the white-to-beige adipocyte conversion occurring in Zfp423-iAKO mice was likewise capable of protecting the animals against diet-induced obesity and impaired glucose tolerance. Starting at 8 weeks of age, Zfp423-iAKO and control mice were administered a high-fat diet (HFD) (60% calories from fat) containing DOX. Body weights of the two groups began to significantly diverge after 11 weeks of HFD feeding, with Zfp423-iAKO mice gaining less weight on the HFD (Figure 3A). Zfp423-iAKO mice weighed significantly less by week 16 of HFD feeding, coinciding with a reduction in WAT depot mass (Figures 3B–3D). Metabolically, the leaner Zfp423-iAKO mice were healthier; these animals were more glucose tolerant and more insulin sensitive than controls (Figures 3E and 3F). Moreover, knockout animals exhibited less hepatic steatosis (Figures 3G and 3H) and significant browning and *UCP1* expression in the iWAT and gWAT, but not the BAT depots (Figures 3I–3K; Figures S5A–S5C). The mRNA levels of inflammatory markers were decreased across all depots examined (Figures S5A–S5C). However, improvements in glucose tolerance and insulin sensitivity can be observed before the divergence in weight again, consistent with the ability of beige adipocytes to elicit beneficial effects on glucose homeostasis independent of its impact on body weight (Figures S5D and S5E) (Seale et al., 2011).

We also assessed the rates of energy expenditure and food intake in control and knockout HFD-fed animals at a time point before the body weights diverged. After 3 weeks of HFD feeding, O_2 consumption and heat production were elevated in the Zfp423-deficient mice (Figures 3L–3O). This increased energy expenditure was observed in the absence of any changes in food intake and locomotor activity (Figures S5F–S5H). This suggests that increased energy expenditure induced by the loss of Zfp423 in mature adipocytes and white-to-beige cell conversion lead to resistance to diet-induced weight gain in these animals. The dependency of these phenotypes on activated beige adipocytes is supported by experiments performed at thermoneutrality. At 30°C, deletion of Zfp423 is sufficient activate the thermogenic gene program to a certain degree (Figure S4); however, the morphological conversion to multilocular cells and resistance to diet-induced obesity are not apparent (Figure S6).

Zfp423 Deficiency, Combined with β3-Adrenergic Receptor Activation, Leads to a Reversal of Weight Gain and Improved Glucose Tolerance when Induced in Obese Animals

The preceding data are in line with numerous mouse models demonstrating that activated beige adipocytes can be protective against weight gain and insulin resistance initiated by HFD feeding. However, it has remained unclear as to whether beige adipocyte activity can be stimulated in the state of obesity (i.e., in animals already obese), leading to a reversal of the metabolic

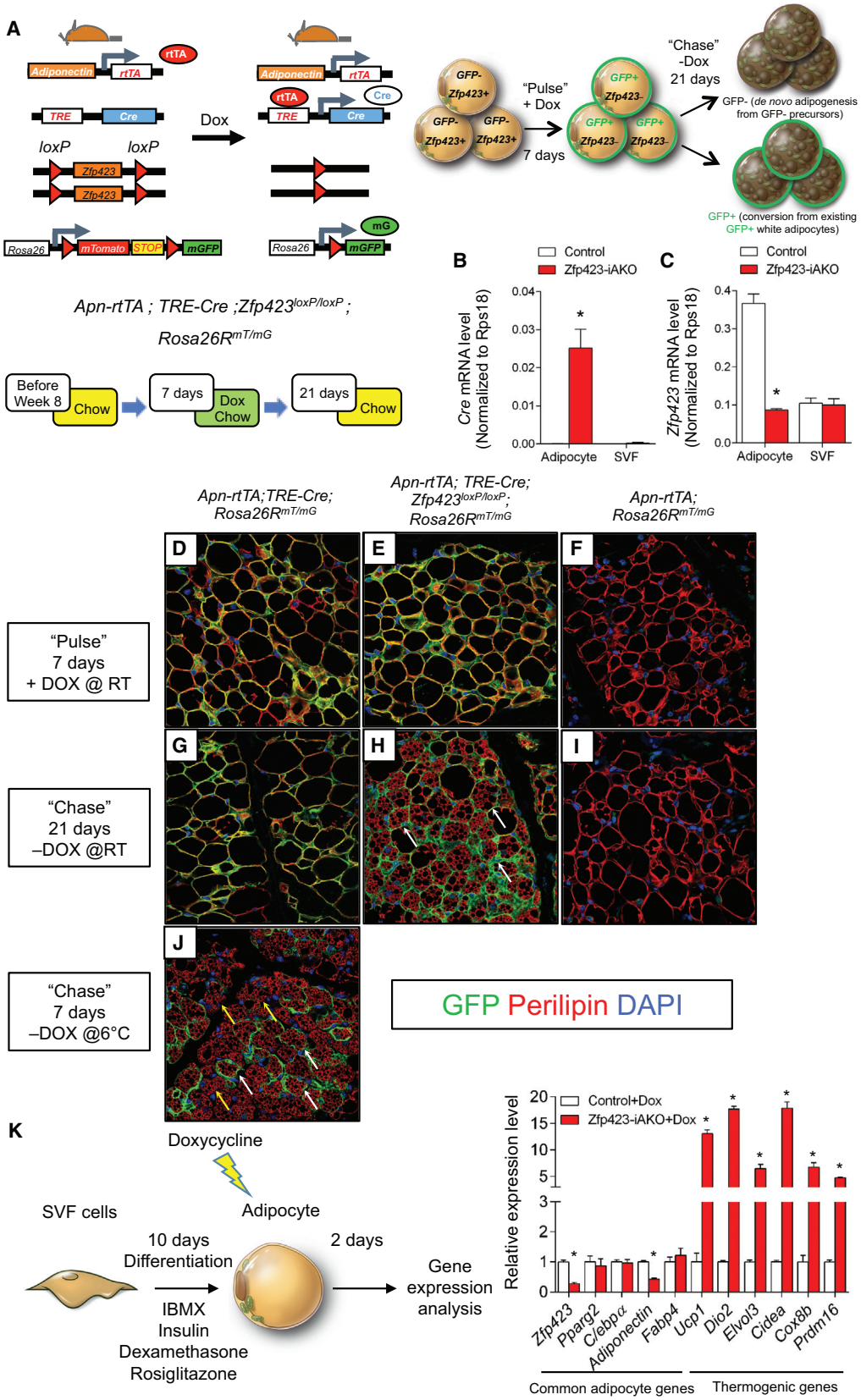

(legend on next page)

dysfunction associated with HFD feeding. Pharmacological approaches and studies have correlated the browning of WAT with improved glucose homeostasis in obese animals; however, direct genetic evidence demonstrating the potential of beige adipocytes in the setting of obesity has been lacking.

We asked whether the deletion of *Zfp423* in mature white adipocytes, and the subsequent beige adipose accumulation, induced in obese animals can lead to the reversal of the weight gain and glucose intolerance triggered by HFD feeding. Following 8 weeks of HFD feeding (without DOX), control and Zfp423-iAKO male mice were switched to HFD feed containing DOX (Figure 4A). Thus, Zfp423 deletion occurs after the mice become obese. Both groups continued to gain weight 1 week after switching the diet. Zfp423-iAKO gained slightly less weight during the next 5 weeks; however, this difference did not reach statistical significance (Figure 4B). We also did not observe any difference in glucose tolerance at this time point (Figure 4C). Gene expression analysis of isolated WAT depots confirmed *Zfp423* inactivation and an induction of the thermogenic gene program (Figures 4D and 4E). Thus, this degree of beige adipose accumulation by itself appears to be insufficient to increase energy expenditure to a significant degree in obese mice.

As described earlier, thermogenic adipocytes rely on β-adrenergic signaling for their activation in vivo. It is well known that obesity is associated with augmented sympathetic activity (Tentolouris et al., 2006). Therefore, we reasoned that the beige cells induced by *Zfp423* deficiency in obese mice would require a stimulus to fully activate their thermogenic function in this setting. To test this, we used subcutaneous osmotic pumps to deliver the β3-adrenergic receptor agonist CL316243 daily at a dose of 1 mg/kg/day for 4 continuous weeks. The agonist was given to obese control and Zfp423 iAKO mice after 14 weeks of HFD feeding (Figure 4A). Control animals were largely resistant to the effects of the β3-receptor agonist. However, Zfp423-iAKO mice given the β3-agonist lost a significant amount of body weight and exhibited markedly improved glucose tolerance after 4 weeks of treatment (Figures 4F and 4G). This was accompanied by reduced hepatic steatosis (Figures 4H–4K) and significant accumulation of beige adipocytes in iWAT (Figures 4L–4Q). The effects on body weight appear to be reversible, because weight rebounded nearly back to baseline after the osmotic pumps released all of their contents (Figure 4F). These data suggest that white adipocytes can be reprogrammed into beige-like adipocytes in obese animals and, when activated, can reverse weight gain and metabolic dysfunction triggered by HFD feeding.

Levels of Zfp423 in Adipocytes Are Suppressed by Cold Exposure or β-Adrenergic Signaling

The robust white-to-beige-like adipocyte conversion in Zfp423-iAKO mice indicates that white adipocytes require *Zfp423* to suppress their thermogenic gene program and maintain a white adipocyte phenotype. This raises the question of whether the suppression of *Zfp423* expression is part of the natural mechanisms by which thermogenic adipocytes accumulate and/or become active under physiological conditions. To address this, we examined protein levels of Zfp423 in WAT and BAT depots of C57BL/6 animals held at room temperature or exposed to 6°C for 3 days. Levels of Zfp423 drop considerably in all depots examined (Figure 5A). The mRNA levels of Zfp423 are suppressed specifically in the adipocyte fraction of adipose tissue in response to cold (Figure 5B). This suppression can occur quickly, within 24 hr of transferring animals from 30°C to 6°C, or in response to β3-adrenergic receptor agonism. Thus, the suppression of adipocyte *Zfp423* expression may allow the transcriptional program regulating adaptive thermogenesis to quickly activate upon cold exposure. The transcriptional response to cold exposure occurs more rapidly and robustly following the inactivation of *Zfp423* in adipocytes of Zfp423-iAKO mice (Figure 5C).

Elevated Zfp423 Expression in Brown Adipocytes Drives a Whitening of BAT

We also assayed the expression of *Zfp423* in settings in which BATs adopt a white adipocyte-like phenotype. In aged animals, BAT depots acquire a white adipose-like phenotype characterized by the increasing presence of unilocular adipocytes and reduction in *UCP1* expression (Figures 5D and 5E). A similar whitening of BAT depots occurs in animals transitioned from room temperature to 30°C (Figures 5F and 5G). We observed that in both settings, the expression of *Zfp423* increases, inversely correlating with *UCP1* expression. These data suggest that the activation of *Zfp423* expression in brown adipocytes can

Figure 2. Beige Adipocytes in Zfp423-iAKO Mice Arise through a Conversion of *adiponectin*$^{+}$ *Zfp423*-Deficient Adipocytes

(A) The Cre-dependent *Rosa26R*$^{mT/mG}$ reporter allele was reconstituted to the Zfp423-iAKO background, allowing for indelible GFP labeling of *Zfp423*-deficient adipocytes. Mice were kept on normal chow until 8 weeks of age before switching to DOX-containing chow for 7 days (pulse). After the labeling period, the mice were switched back to a standard chow diet (devoid of DOX) for another 21 days (chase). After the 21-day period, the presence of GFP^{-} multilocular adipocytes indicates beige cells were derived from GFP^{-} precursors. The presence of GFP^{+} multilocular adipocytes indicates beige cells that arise directly from mature adipocytes targeted during the pulse-labeling period.

(B and C) mRNA levels of (B) *Cre* and (C) *Zfp423* in purified adipocytes and SVF from iWAT of control and Zfp423-iAKO mice after 7 days of DOX feeding. n = 4.

(D–F) Representative immunofluorescence staining of Perilipin (red) and GFP (green) in iWAT sections obtained from (D) control mice (*Adpn*-rtTA; TRE-Cre; *Rosa26R*$^{mT/mG}$), (E) Zfp423-iAKO mice (*Adpn*-rtTA; TRE-Cre; *Zfp423*$^{loxP/loxP}$; *Rosa26R*$^{mT/mG}$), and (F) additional control mice (*Adpn*-rtTA; *Rosa26R*$^{mT/mG}$) after pulse labeling (pulse).

(G–I) Representative immunofluorescence staining of Perilipin (red) and GFP (green) in iWAT sections obtained from (G) control mice, (H) Zfp423-iAKO mice, and (I) additional control mice held at room temperature (RT) for 21 days after the removal of DOX (chase). White arrows in (H) denote GFP^{+} adipocytes.

(J) Representative immunofluorescence staining of Perilipin (red) and GFP (green) in iWAT sections obtained from control mice exposed to cold temperatures (6°C) for 7 days after the removal of DOX (chase). White arrows denote GFP^{+} adipocytes, and yellow arrows denote GFP^{-} adipocytes.

(K) iWAT SVF isolated from control and Zfp423-iAKO mice were induced to differentiate in vitro. After differentiation, the adipocytes were treated with 5 μM DOX for 12 hr. Relative mRNA levels of common adipocyte genes and thermogenic genes were measured by qPCR in the differentiated adipocytes 2 days after DOX treatment. n = 3.

Student's t test, *$p < 0.05$.

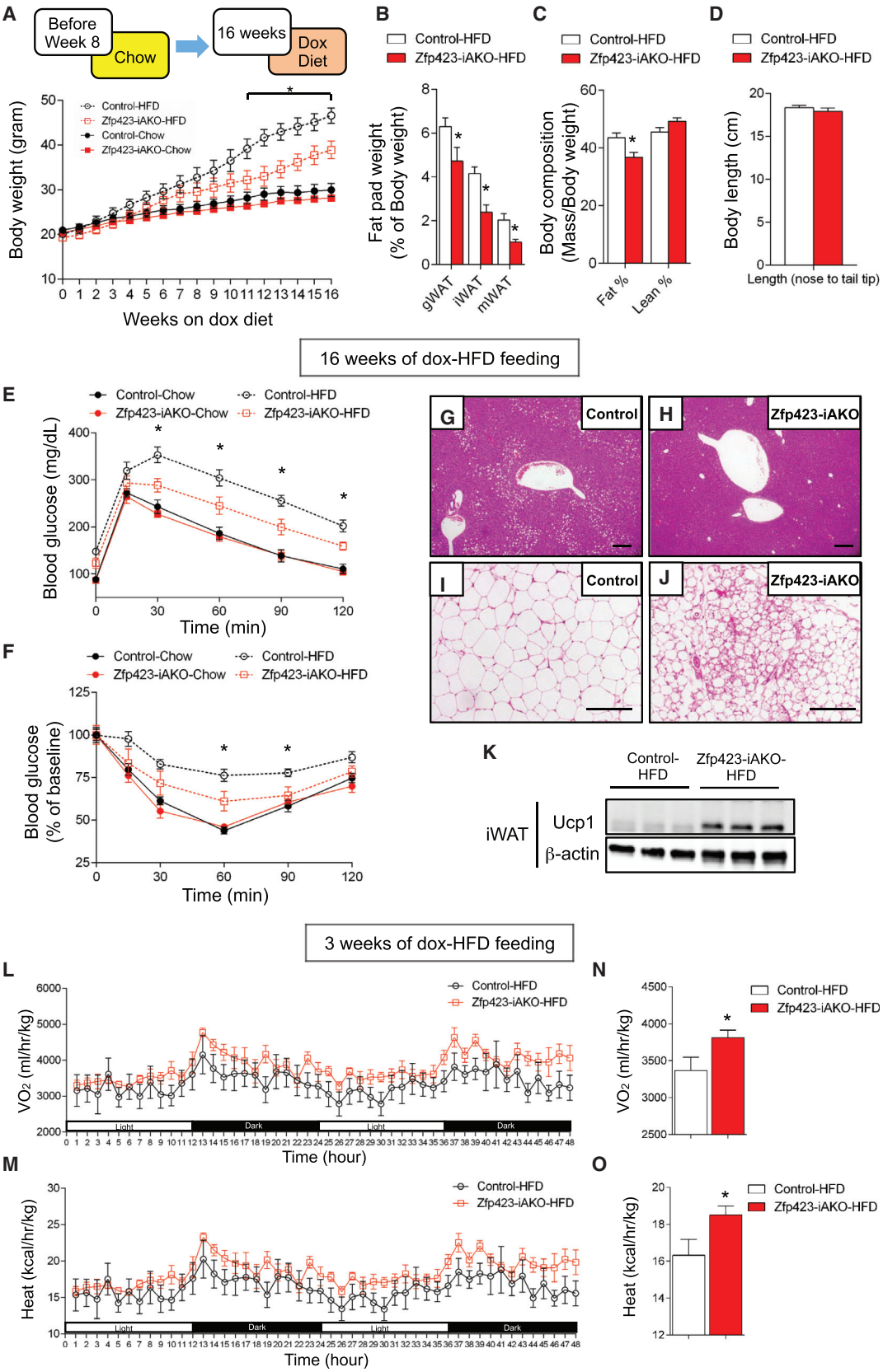

(legend on next page)

switch cells to a more white-like phenotype. We tested this hypothesis directly by generating a transgenic model in which *Zfp423* expression can be induced in *adiponectin*$^{+}$ adipocytes in the presence of DOX. This bi-transgenic model consists of the aforementioned *adiponectin* promoter-driven rtTA allele (*Adiponectin*^{rtTA}) and a transgenic allele in which full-length *Zfp423* (ZF 1–30) is expressed from a promoter containing the TRE (*Adiponectin*^{rtTA}; TRE-Zfp423, herein Zfp423-AOE) (Figure 5H). As described earlier and previously reported, activity of the *Adiponectin*^{rtTA} transgene is relatively weak in adult brown adipocytes (Wang et al., 2013). As a result, we achieve modest, but physiological, overexpression of *Zfp423* in BAT of transgenic adult mice at room temperature. Levels of *Zfp423* are induced in BAT to a level that is only a fewfold higher than what is observed in BAT of animals housed at thermoneutrality (Figure 5I). Strikingly, ~7-fold overexpression of Zfp423 is sufficient to drive a conversion of BAT to a more unilocular white adipocyte-like phenotype at room temperature (Figures 5J and 5K). Expression of pan-adipocyte selective genes is not affected; however, the thermogenic gene program is largely suppressed (~70%–80% reduction in *UCP1* mRNA), while expression of white adipocyte-selective genes is induced (Figure 5L). In cold-exposed Zfp423-AOE mice, *UCP1* expression was not affected by the Zfp423 transgene; however, transgene activity was noticeably weaker under these conditions (Figure S7). Overexpression of Zfp423 in iWAT is also modest (~4-fold). However, this level is sufficient to partially inhibit browning of the iWAT depot in animals exposed to cold (Figure S7). Together, these data indicate that Zfp423 acts as a dominant suppressor of the thermogenic gene program in mature adipocytes. The data suggest that a doubling of *Zfp423* expression in brown adipocytes, combined with a gradual age-related reduction in sympathetic tone, may contribute to the natural age-related alterations in BAT phenotype.

Zfp423 Suppresses the Thermogenic Gene Program in White Adipocytes through Repression of Ebf2 Transcriptional Activity

Zfp423 is a multi-ZF protein that contains 30 C2H2 ZF motifs, organized into five distinct domains (Figure 6A) (Tsai and Reed, 1998). We previously mapped the ZF domains critical for the ability of Zfp423 to enhance BMP-induced adipogenesis and *Pparγ* expression in cultured cells (Gupta et al., 2010). This function was found to be dependent on its ability to interact with Smad proteins (ZF 14–20). We sought to elucidate the mechanism by which Zfp423 suppresses the thermogenic gene program by using a similar domain-mapping approach. We used retroviral vectors to express ZF 1–30, a variant incapable of Smad interaction (ΔSBD), or a previously described variant lacking the C-terminal ZFs (ZF 1–25) (Figure 6A) (Hata et al., 2000). Primary brown stromal vascular cultures transduced with these viruses all differentiated into adipocytes to a similar degree (Figures 6B and 6C). However, cells expressing ZF 1–30 adopted a white adipocyte-like gene expression profile; levels of *Ucp1* and other thermogenic genes were significantly lower than those of control cultures (Figure 6D). This effect was not dependent on Smad-protein interactions, because expression of a mutant Zfp423 lacking the Smad-binding domain (ΔSBD; ZF 14–20) was equally effective in suppressing thermogenic gene expression. However, expression of a variant of Zfp423 lacking the C-terminal ZFs (ZF 26–30) was entirely ineffective at suppressing the thermogenic genes (Figure 6D), despite being expressed at levels similar to those of ZF 1–30 or ΔSBD (Figure 6A). This indicates that the ability of Zfp423 to suppress brown adipocyte phenotype in cells is dependent on the C-terminal ZF domain. Moreover, this suggests that the mechanism by which Zfp423 functions in precursors to promote adipogenesis is distinct from the mechanism it employs to inhibit the thermogenic gene program.

Zfp423 was originally cloned as an interacting partner of the Ebf family of transcription factors in the olfactory epithelium; ZF 28–30 of Zfp423 mediates this direct interaction (Tsai and Reed, 1997). We confirmed that this interaction could occur in differentiated white adipocytes (Figure 7A). As described earlier, the Ebf2 family member is required for the development of brown and beige adipocytes. The ability of Zfp423 to suppress the thermogenic gene program in white adipocytes is dependent on the same ZFs that mediate its potential to interact with Ebf proteins; therefore, we postulated that Zfp423 functions in white adipocytes to control Ebf2 activity.

The iWAT stromal vascular cultures transduced with Ebf2-expressing retrovirus differentiate into brown-like adipocytes (Figure 6E) (Rajakumari et al., 2013). However, co-expression of Zfp423 in Ebf2-expressing cells strongly inhibits the induction of *Prdm16* and the thermogenic gene program, even though it has no discernible effect on overall adipocyte differentiation

Figure 3. Mice Lacking Adipocyte Zfp423 Are Resistant to Diet-Induced Obesity

(A) Control and Zfp423-iAKO mice were fed a standard chow diet until 8 weeks of age before switching to DOX-containing chow or DOX-containing HFD (DOX-HFD). Body weights of control and Zfp423-iAKO mice were measured weekly. Two-way ANOVA, *p < 0.05, control-HFD versus Zfp423-iAKO-HFD, n = 6–8.

(B) Fat pad weight (normalized to body weight) of control and Zfp423-iAKO mice after 16 weeks of DOX-HFD feeding. Student's t test, *p < 0.05, n = 6.

(C) Total fat mass and lean mass (normalized to body weight) of control and Zfp423-iAKO mice after 16 weeks of DOX-HFD feeding. Student's t test, *p < 0.05, n = 12–13.

(D) Body length of control and Zfp423-iAKO mice after 16 weeks of DOX-HFD feeding. n = 6.

(E and F) Glucose tolerance test (E) and insulin tolerance test (F) of control and Zfp423-iAKO mice after 16 weeks of DOX feeding. Two-way ANOVA, *p < 0.05, control-HFD versus Zfp423-iAKO-HFD, n = 6–8.

(G and H) Representative H&E staining of liver of (G) control mice and (H) Zfp423-iAKO mice after 16 weeks of DOX-HFD feeding. Scale bar, 200 μM.

(I and J) Representative H&E staining of iWAT from (I) control mice and (J) Zfp423-iAKO mice after 16 weeks of DOX-HFD feeding. Scale bar, 200 μM.

(K) Western blot of Ucp1 protein levels in iWAT of control and Zfp423-iAKO mice after 16 weeks of DOX-HFD feeding.

(L and M) O_2 consumption (L) and heat production (M) in control and Zfp423-iAKO mice during two complete 12 hr light-dark cycles following 3 weeks of DOX-HFD feeding. n = 6.

(N and O) Average O_2 consumption (N) and average heat production (O) of control and Zfp423-iAKO mice during the 5-day measurement. Student's t test, *p < 0.05, n = 6.

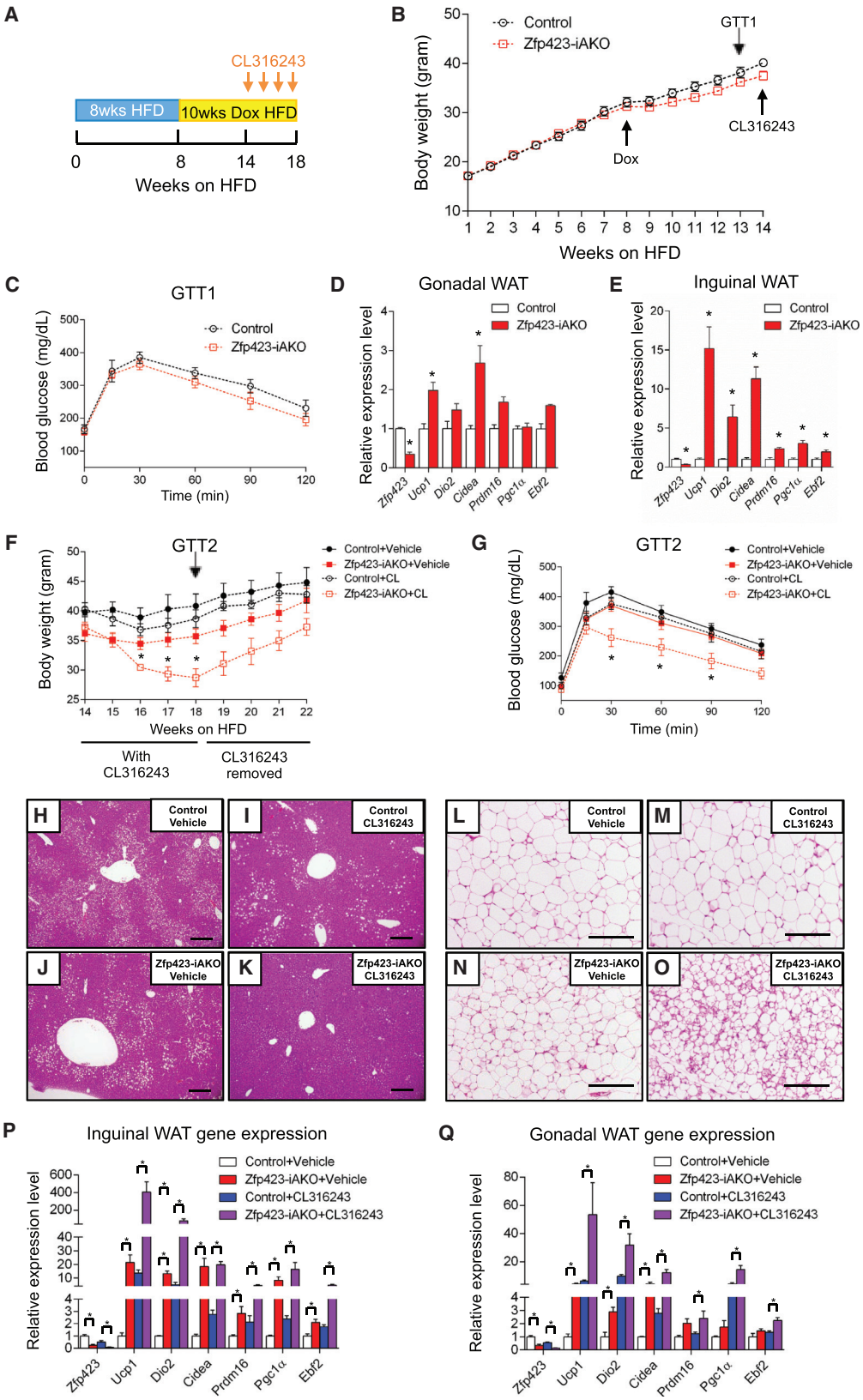

(legend on next page)

(Figure 6E). This suggests that Zfp423 inhibits the transcriptional activity of Ebf2. We tested this directly by employing classic luciferase-based gene reporter assays. Ebf2 alone, or in conjunction with Pparγ/RXRα heterodimers, binds and activates an Ebf2-dependent enhancer element located at the *Prdm16* locus (Figure 6F) (Rajakumari et al., 2013). Co-transfection of Zfp423 with Ebf2 or Ebf2/Pparγ/RXRα abolishes the ability of Ebf2 to activate the *Prdm16* enhancer element (Figure 6F). This suggests a model in which Zfp423 serves as a transcriptional co-repressor of Ebf2 activity in white adipocytes; inactivation of Zfp423 then results in increased Ebf2-mediated induction of *Prdm16* and the beige adipocyte gene program. In support of this model, CRISPR-Cas9-mediated inactivation of *Ebf2* in *Zfp423*-deficient adipocyte cultures largely prevents the induction of the beige cell phenotype (Figures 6G and 6H). These data indicate that the white-to-beige fat cell conversion induced by Zfp423 inactivation is dependent on Ebf2.

Activation of BMP Signaling in Adipocytes Disrupts the Interaction between Zfp423 and Ebf2

As described earlier, Zfp423 expression is regulated in a depot- and temperature-dependent manner. Brown adipocytes express relatively lower levels of Zfp423 than do white adipocytes; however, protein levels remain detectable and are not entirely lost upon cold exposure. Thus, we reasoned that mechanisms beyond the control of gene expression might exist to alter Zfp423 function in adipocytes. The robust conversion of the white-to-beige adipocytes in the absence of Zfp423, and the dependence of this phenotype on Ebf2, prompted us to ask whether natural or pharmacological signals that promote beige and/or brown adipocyte development modulate the interaction between these two proteins. We treated differentiated adipocyte cultures with ligands that promote activation of the thermogenic gene program. Pparγ agonism (rosiglitazone) or adrenergic receptor activation (isoproterenol) did not affect the interaction between virally expressed Zfp423 and Ebf2, at least under the conditions used here. However, treatment with BMP7, and to a lesser extent BMP4, reduced the degree of interaction between Ebf2 and Zfp423 (Figure 7B). The strong effect elicited by BMP7 is noteworthy, because there is considerable evidence pointing to BMP7 signaling as a key determinant of brown adipocyte development, triggering brown adipogenesis through a number of mechanisms (Tseng et al., 2008). Canonical BMP signaling leads to the activation of Smad1/4-mediated transcription. As described earlier, BMP signaling in the adipose lineage activates *Pparγ* expression and adipogenesis; Zfp423 serves as the Smad co-activator and amplifies the pro-adipogenic effects of BMPs (Gupta et al., 2010). Accordingly, BMP7 treatment triggers an interaction between Zfp423 and Smad1/4 (Figure 7C). The interaction between Ebf2 and ΔSBD is not inhibited by BMP treatment (Figure 7C). This indicates that BMP7 disrupts the Zfp423-Ebf2 complex through induction of a Zfp423-Smad complex and provides evidence of cross-talk between BMP7 signaling and Ebf2 signaling pathways in the formation of thermogenic adipocytes. These data suggest that Zfp423 activity can be controlled at the transcriptional and post-translational level by physiological stimuli of brown adipocyte development and thermogenic gene activation.

DISCUSSION

Tremendous progress has been made in identifying transcriptional components functioning within the brown or beige adipocyte lineage that either positively or negatively affect the differentiation of their respective precursors. As described earlier, Prdm16 and Ebf2 are among a growing group of factors that drive the activation of the thermogenic gene program. Inhibitors of brown and beige cell precursor differentiation have also been described, including Rb/p107, MTFRA, and TLE3 (De Sousa et al., 2014; Hansen et al., 2004; McDonald et al., 2015; Villanueva et al., 2013). TLE3, similar to Zfp423, promotes adipocyte differentiation though activation of *Pparγ* while suppressing Prdm16 activity and the thermogenic gene program (Villanueva et al., 2011, 2013). The precise step in the adipose lineage affected by TLE3 and these other proteins is not entirely clear; however, many of these factors appear to function at the level of the brown or beige precursor to effect lineage commitment and/or differentiation. Here, we reveal a mechanism that acts at the level of a fully mature white adipocyte to suppress the thermogenic gene program characteristic of brown and beige fat cells.

We previously identified Zfp423 as a molecular marker and functional regulator of committed preadipocytes. Zfp423 regulates preadipocyte levels of *Pparγ* and is required for proper

Figure 4. Reversal of Weight Gain and Glucose Intolerance by Inducible Inactivation of Adipocyte Zfp423 in Obese Mice

(A) Obesity was induced in 5-week-old control and Zfp423-iAKO mice by administering a HFD for 8 weeks. Then, animals were switched to a DOX-containing HFD (DOX-HFD) for another 14 weeks. After 5 weeks of DOX-HFD, the mice were treated daily with CL316243 (1 mg/kg/24 hr) or vehicle (PBS) for 4 weeks via osmotic pumps.

(B) Body weights of control and Zfp423-iAKO mice before CL316243 administration. n = 12–13.

(C) Glucose tolerance test (GTT) of control and Zfp423-iAKO mice immediately before CL316243 administration. n = 6–7.

(D and E) Relative mRNA levels of indicated genes in (D) gWAT and (E) iWAT from DOX-HFD-fed control and Zfp423-iAKO mice before CL316243 administration. Student's t test, *p < 0.05, n = 4–5.

(F) Body weights of control and Zfp423-iAKO mice after vehicle or CL316243 administration. Two-way ANOVA, *p < 0.05, control-CL316243 versus Zfp423-iAKO-CL316243, n = 5–9.

(G) Glucose tolerance test (GTT) of control and Zfp423-iAKO mice after vehicle or CL316243 administration. Two-way ANOVA, *p < 0.05, control-CL316243 versus Zfp423-iAKO-CL316243, n = 5.

(H–K) Representative H&E staining of the liver from (H) control mice receiving vehicle treatment (week 18 of HFD, as indicated in A), (I) control mice receiving CL316243, (J) Zfp423-iAKO mice receiving vehicle, and (K) Zfp423-iAKO mice receiving CL316243. Scale bar, 200 μM.

(L–O) Representative H&E staining of iWAT from (L) control mice receiving vehicle treatment (week 18 of HFD, as indicated in A), (M) control mice receiving CL316243, (N) Zfp423-iAKO mice receiving vehicle, and (O) Zfp423-iAKO mice receiving CL316243. Scale bar, 200 μM.

(P and Q) Relative mRNA levels of indicated genes in (P) iWAT and (Q) gWAT from control and Zfp423-iAKO mice after vehicle or CL316243 administration. (week 18 of HFD, as indicated in A). Two-way ANOVA,*p < 0.05, n = 5.

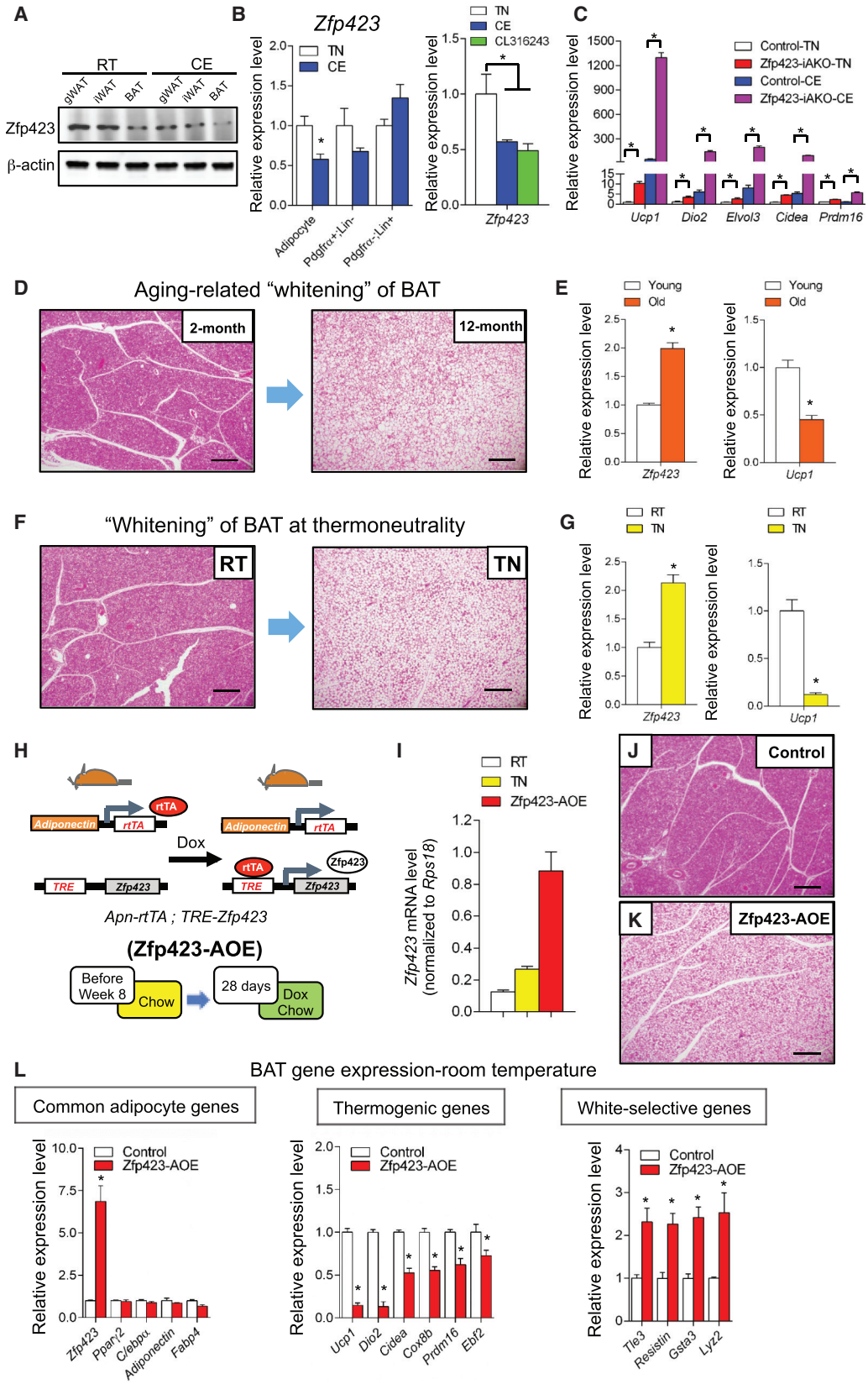

(legend on next page)

white and brown adipocyte differentiation in vitro and in vivo. The expression of *Zfp423* persists throughout adipocyte differentiation; therefore, in designing these experiments, we initially hypothesized that *Zfp423* would also be required to maintain *Pparγ* expression, and thus the general adipocyte gene program, in mature adipocytes. On the contrary, our data reveal that *Zfp423* is dispensable for maintaining the adipocyte identity per se. Other known regulators of *Pparγ* expressed in mature fat cells, such as C/ebp family members, may collectively compensate for the loss of Zfp423 to maintain adipocyte *Pparγ* gene expression. Instead, Zfp423 functions in mature white adipocytes to suppress the thermogenic gene program associated with beige and/or brown adipocytes. The dual roles for Zfp423 in the adipose lineage are seemingly disparate. However, taken together, the data on *Zfp423* implicate this factor as a white adipocyte determination factor; Zfp423 regulates the initial formation of a white adipocyte and later plays a role in maintaining the energy-storing, or white, phenotype of WAT.

Lineage-tracing studies using the same inducible system applied here have definitively established that cold-induced beiging occurs by de novo differentiation from precursors (*adiponectin*$^-$ cells) and, to a lesser degree, by Ucp1 activation in existing *adiponectin*$^+$ adipocytes. Kajimura et al. (2015) synthesized the available data and proposed a model in which at least two general mechanisms lead to the natural formation of beige adipocytes during cold exposure: (1) de novo differentiation from precursors (*adiponectin*$^-$ cells) and (2) activation of dormant unilocular beige adipocytes (*adiponectin*$^+$ cells) that were present from prior cold exposure. Our lineage-tracing data indicate that the beige-like adipocytes that accumulate in Zfp423-iAKO mice originate from *adiponectin*$^+$ adipocytes through a lineage conversion. These *adiponectin*$^+$ adipocytes may represent dormant beige adipocytes being activated by *Zfp423* deletion or bona fide white adipocytes that are being reprogrammed. The browning we observe in our animals is widespread and can be triggered in all major WAT depots, even those relatively resistant to cold-induced browning. Thus, a reprogramming of bona fide white adipocytes is likely occurring in this model. The accepted model of physiological white adipose browning highlights the importance of de novo beige adipogenesis; however, our data highlight the potential for white adipocytes in obesity to activate a thermogenic program when the brake is removed.

Levels of *Zfp423* appear to be regulated physiologically in settings in which the thermogenic potential of adipocytes is altered. *Zfp423* expression in vivo is suppressed in mature adipocytes upon cold exposure or pharmacological activation of β3-adrenergic receptors. This regulation happens quickly (1 day of cold), and we observe this at the protein and mRNA levels. This suppression of *Zfp423* occurs in BAT, likely contributing to the activation of the thermogenic program in this depot. Downregulation of Zfp423 also happens in inguinal adipocytes, likely in pre-existing dormant beige cells that activate Ucp1 or even in newly formed beige adipocytes originating in response to cold exposure. This also happens in gWAT, a depot relatively resistant to browning. As highlighted here, cells of this depot require additional stimuli to fully activate their thermogenic capacity, even in the absence of Zfp423. Moreover, we find that *Zfp423* expression in BAT increases in settings in which whitening of BAT occurs and that expression of Zfp423 in brown adipocytes is sufficient to suppress Ucp1 and other genes of the thermogenic program. Together, these data reveal that the suppression of Zfp423 is part of the normal physiology of cold-induced browning. However, the loss of function data show that Zfp423 is a major part of the normal physiology of how adipocytes stay or become white.

In the model we propose, Zfp423 suppresses the thermogenic gene program in adipocytes by antagonizing the actions of Ebf2, a brown fat determination factor (Figure 7D). Our cellular experiments indicate that Zfp423 inhibits the ability of Ebf2 to convert white stromal cells into beige adipocytes. This interaction seems important, because the ability of Zfp423 to suppress the thermogenic gene program is dependent on its Ebf-interaction domain. Moreover, depletion of Ebf2 in Zfp423-deficient adipocyte cultures largely blocks the induction of the thermogenic gene program. Inhibition of Ebf2 likely explains how Zfp423 suppresses the thermogenic gene program in BAT and iWAT; however, gWAT naturally expresses lower levels of Ebf2. The highly related Ebf1 is present in gWAT and is capable of driving brown and/or beige adipocyte gene expression (Rajakumari et al., 2013). Thus, Zfp423 may function in this depot through inhibition of Ebf1 rather than Ebf2. It is also possible that Zfp423 functions through additional mechanisms that remain unidentified.

Figure 5. Physiological Regulation of Brown and White Adipocyte *Zfp423* Expression

(A) Western blot of endogenous Zfp423 proteins in adipose depots isolated from C57BL/6 mice held at room temperature (RT) or exposed to cold (6°C) (CE) for 3 days.

(B) Left: relative mRNA levels of *Zfp423* in fractionated iWAT adipocytes, Pdgfrα+; Lin− (CD31− and CD45−) cells, and Pdgfrα−; Lin+ (CD31+ and CD45+) cells isolated from C57BL/6 mice held at thermoneutrality (TN) or CE for 3 days. Right: relative mRNA levels of *Zfp423* in iWAT isolated from C57BL/6 mice held at TN, CE for 1 day, or injected with CL316243 (1 mg/kg/day) for 3 days. One-way ANOVA or Student's t test, *$p < 0.05$, n = 4–6.

(C) Relative mRNA levels of *Zfp423* and thermogenic genes in iWAT of control and Zfp423-iAKO mice held at TN or CE for 1 day. Two-way ANOVA, *$p < 0.05$, n = 5.

(D) Representative H&E staining of interscapular BAT from 2-month-old and 12-month-old C57BL/6 mice. Scale bar, 200 μM.

(E) Relative mRNA levels of *Zfp423* and *Ucp1* in interscapular BAT from 2-month-old and 12-month-old C57BL/6 mice. Student's t test, *$p < 0.05$, n = 6.

(F) Representative H&E staining of interscapular BAT from C57BL/6 mice held at RT or TN. Scale bar, 200 μM.

(G) Relative mRNA levels of *Zfp423* and *Ucp1* in interscapular BAT from C57BL/6 mice held at RT or TN. Student's t test, *$p < 0.05$, n = 6.

(H) Animals conferring adipocyte-specific Zfp423 overexpression (Zfp423-AOE mice) were derived by breeding *Adiponectin*^{rtTA} transgenic mice with transgenic mice expressing full-length murine *Zfp423* under the control of a promoter containing TRE-Cre (*TRE-Zfp423*). Littermates carrying only the *Adiponectin*^{rtTA} allele were used as control animals. Mice were kept at RT and fed standard chow until 8 weeks of age before switching to DOX-containing chow diet for another 28 days.

(I) mRNA levels of *Zfp423* in BAT of C57BL/6 mice held at RT or TN and BAT of Zfp423-AOE mice held at RT. n = 4–6.

(J and K) Representative H&E staining of BAT from (J) control mice and (K) Zfp423-AOE mice after DOX feeding. Scale bar, 200 μM.

(L) Relative mRNA levels of common adipocyte genes, thermogenic genes, and white adipocyte-selective genes in BAT of control and Zfp423-AOE mice after DOX feeding. Student's t test, *$p < 0.05$, n = 4.

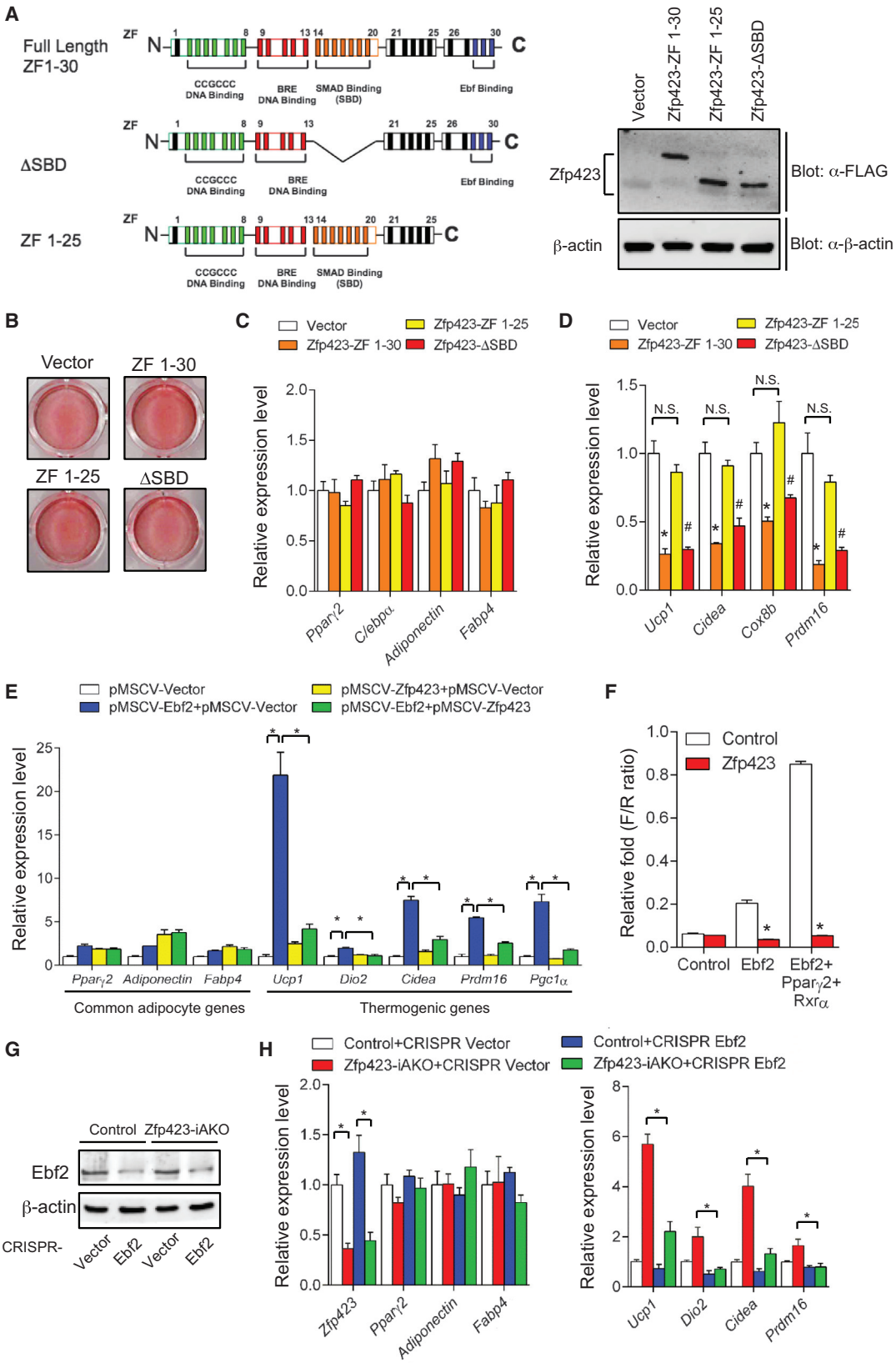

(legend on next page)

The suppression of *UCP1* by transgenic *Zfp423* expression in classical brown adipocytes is somewhat surprising, given that BAT development is significantly impaired in *Zfp423*-deficient embryos and that Zfp423 is expressed to some degree in brown and beige cell precursors (Gupta et al., 2010, 2012). However, the mechanisms by which Zfp423 regulates adipocyte differentiation per se and thermogenic gene regulation are distinct. Moreover, the interaction between Zfp423 and Ebf2 appears to be inhibited by at least some signals that promote brown and/or beige adipogenesis. These data offer a model for how Zfp423 can regulate *Pparγ* expression and adipogenesis in the brown adipose lineage but not inhibit Ebf2 function and the thermogenic gene program (Figure 7E). BMP7 in particular is a potent driver of brown adipocyte differentiation, both regulating *Pparγ* expression and activating *Prdm16*. A number of mechanisms have been put forth to explain the actions of BMP7 in brown adipocytes (Townsend et al., 2013; Zhang et al., 2010). Our data provide an additional possibility that involves Zfp423-mediated cross-talk between BMP or Smad signaling and Ebf2 signaling.

The recent discoveries of active brown and beige adipocytes in adult humans have renewed the interest in elucidating the mechanisms controlling the formation of these cells and deriving novel strategies to stimulate their activity as a treatment for metabolic disease. It has remained unclear as to whether the numbers of beige or brown adipocytes present in obese individuals are sufficient to increase energy expenditure therapeutically. The data presented here indicate that loss of *Zfp423*, combined with pharmacological stimulation, is sufficient to unlock the thermogenic potential of existing white adipocytes in the setting of obesity. Thus, direct programming of white adipocytes into beige-like cells may be an effective strategy to increase the supply of beige adipocytes in obese individuals. Our observation that natural brown adipocyte differentiation factors, such as BMPs, disrupt the anti-thermogenic Zfp423-Ebf2 complex suggests a plausible therapeutic strategy to trigger this reprogramming event. Further insight into the regulation of adipocyte *Zfp423* expression, as well as its regulation and function in other adult tissues, may lead to novel strategies to combat obesity and metabolic disease.

EXPERIMENTAL PROCEDURES

Mice

The *Adiponectin*^{rtTA} transgenic line was a gift of P. Scherer (University of Texas Southwestern Medical Center, or UTSW) and previously described (Wang et al., 2013). TRE-Cre transgenic mice and the Rosa26-loxP-stop-loxP-Lacz reporter line were obtained from Jackson Laboratory. *Zfp423*$^{loxP/loxP}$ mice were a gift from Dr. S. Warming (Genentech) (Warming et al., 2006). TRE-Zfp423 transgenic mice were derived by the UTSW transgenic core facility as described in the Supplemental Information. Mice were maintained at room temperature or at 6°C when indicated, with a 12 hr light-dark cycle and free access to food and water. All animal experiments were performed according to procedures approved by the UTSW Institutional Animal Care and Use Committee. Metabolic cage studies were conducted using a Comprehensive Lab Animal Monitoring System (CLAMS, Columbus Instruments) at the UTSW Metabolic Phenotyping Core. Further details of CLAMS analysis can be found in the Supplemental Experimental Procedures.

Histological Analysis

Tissues were dissected and fixed in 4% paraformaldehyde overnight. Paraffin processing, embedding, sectioning, and standard H&E staining were performed at the Molecular Pathology Core Facility at UTSW. Detailed protocols for indirect immunofluorescence can be found in the Supplemental Experimental Procedures.

Isolation of Adipose SVF and In Vitro Differentiation

SVF cells isolated by collagenase digestion of minced WAT or BAT (see Supplemental Experimental Procedures) were plated onto collagen-coated dishes and cultured in 10% CO_2 at 37°C. WAT SVF cells were expanded in growth media containing DMEM/F12 (Invitrogen) and 10% fetal bovine serum (FBS). BAT SVF cells were maintained in growth media containing high-glucose DMEM (Invitrogen) supplemented with 20% FBS and 20 mM HEPES (ph 7.4). For white adipocyte differentiation, confluent cultures were stimulated with an adipogenic cocktail (growth media supplemented with 5 μg ml^{-1} insulin, 1 μM dexamethasone, 0.5 mM isobutylmethyxanthine, and 1 μM rosiglitazone) for 48 hr. After 48 hr, the cells were maintained in growth media supplemented with 5 μg ml^{-1} insulin until harvest. For brown adipocyte differentiation, confluent cultures were stimulated with an adipogenic cocktail (high-glucose DMEM media supplemented with 10% FBS, 20 mM HEPES [pH 7.4], 10 nM tri-iodothyronine, 0.1 mg ml^{-1} insulin, 1 μM dexamethasone, 0.5 mM isobutylmethyxanthine, and 0.125 mM indomethacin) for 48 hr. After 48 hr, the cells were maintained in maintenance media (high-glucose DMEM media supplemented with 10% FBS, 20 mM HEPES [pH 7.4], 10 nM tri-iodothyronine, and 0.1 mg ml^{-1} insulin) until harvest.

Gene Expression Analysis

Total RNA from tissue or cultured cells was extracted and purified using the TRIzol reagent (Invitrogen) and the RNeasy Mini Kit (QIAGEN). cDNA was synthesized with M-MLV reverse transcriptase (Invitrogen) and random hexamer primers (Invitrogen). Relative expression of mRNAs was determined by qPCR using the SYBR Green PCR system (Applied Biosystems), and values were normalized to ribosomal protein S18 (Rps18) levels using the ΔΔ-Ct method. All primer sequences are provided in Table S2. Global gene expression profiling by Affymetrix microarray analysis was conducted at the UTSW Genomics and Microarray Core. Total RNA samples from iWAT were hybridized to GeneChip Mouse Transcriptome Assay v.1.0 (Affymetrix) according to the manufacturer's protocols. Normalization and statistical analysis were

Figure 6. Zfp423 Suppresses the Thermogenic Gene Program in White Adipocytes through Repression of Ebf2 Transcriptional Activity

(A) Left: schematic illustration of ZF 1–30, ΔSBD, and the Zfp423 C-terminal mutant (ZF 1–25). Right: western blots of FLAG-tagged Zfp423 protein levels of in vitro differentiated primary brown adipocytes expressing ZF 1–30 and Zfp423 mutants.

(B) Oil red O staining of in vitro differentiated brown adipocytes expressing ZF 1–30 and Zfp423 mutants.

(C and D) Relative mRNA levels of common adipocyte genes (C) and thermogenic genes (D) of in vitro differentiated brown adipocytes expressing ZF 1–30 and Zfp423 mutants. One-way ANOVA, *p < 0.05, vector versus ZF 1–30; #p < 0.05, vector versus ZF 1–ΔSBD; NS, not significant; n = 3.

(E) Relative mRNA levels of common adipocyte genes and thermogenic genes of in vitro differentiated iWAT adipocytes virally expressing Zfp423, Ebf2, or Zfp423 and Ebf2. One-way ANOVA, *p < 0.05, n = 3.

(F) Firefly luciferase activity (normalized to Renilla activity) in cells transfected with the *Prdm16* enhancer-driven firefly luciferase reporter construct and Ebf2 or Ebf2/Pparγ/Rxrα vectors, with or without Zfp423 co-expression. Student's t test, *p < 0.05, n = 3.

(G) iWAT SVF cells were isolated from control and Zfp423-iAKO mice and transduced with the indicated CRISPR lentivirus before in vitro differentiation. Ebf2 protein levels in the differentiated adipocyte cultures were detected by western blotting.

(H) Relative mRNA levels of common adipocyte genes and thermogenic genes of in vitro differentiated iWAT adipocytes with indicated genotype and CRISPR lentivirus transduction. Two-way ANOVA, *p < 0.05, n = 3.

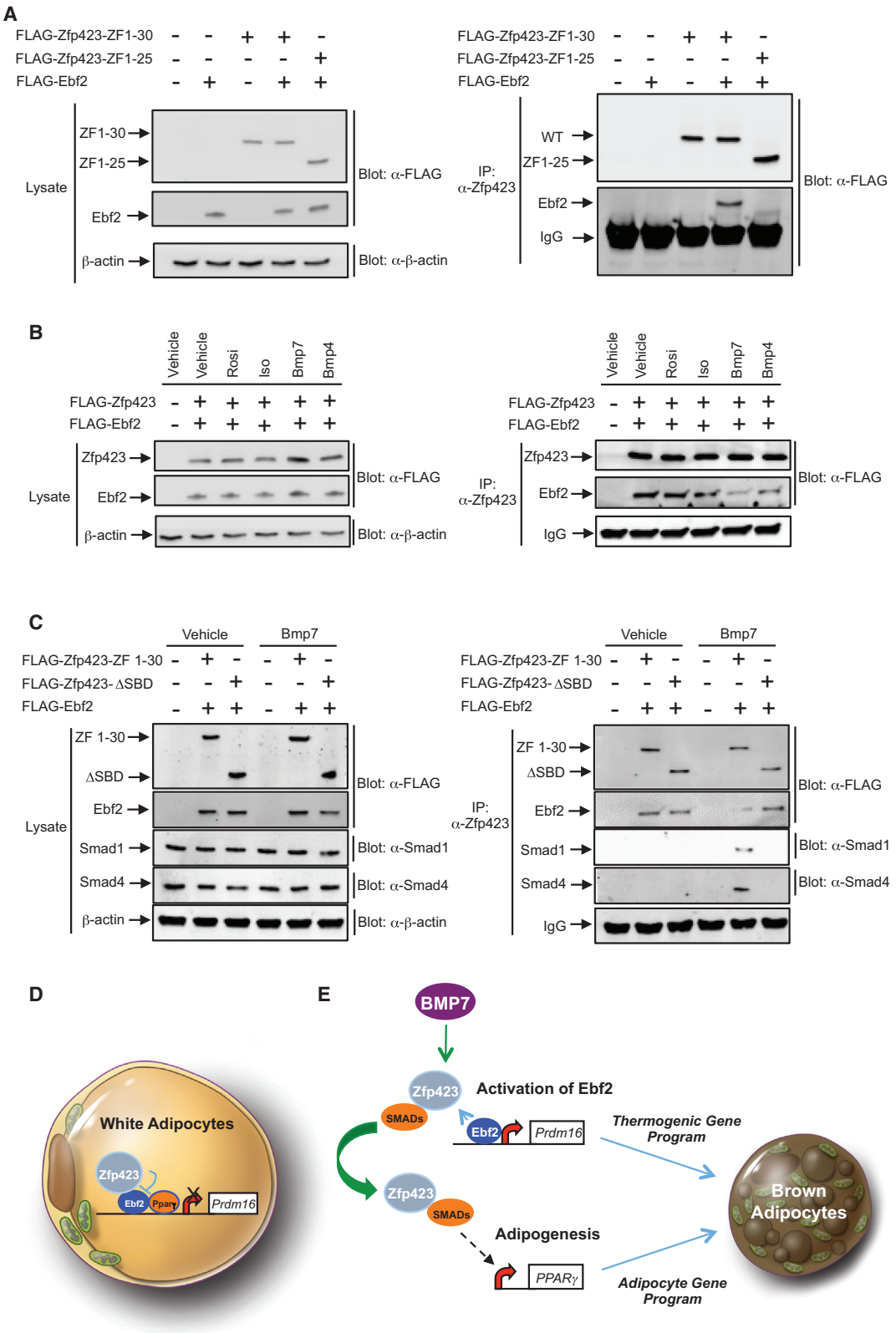

(legend on next page)

performed using Transcriptome Analysis Console v.3.0 (Affymetrix). Gene ontology analysis was performed using the NIH database for annotation, visualization, and integrated discovery (DAVID). All microarray data have been deposited to GEO: GSE74899.

Plasmids and Retrovirus Production

Retroviruses were constructed using the pMSCV viral backbone (Clontech Laboratories). The pMSCV Zfp423 full-length, pMSCV Zfp423 ΔSBD, and pMSCV Ebf2 plasmids were described previously (Gupta et al., 2010; Rajakumari et al., 2013). The Ebf-binding mutant of Zfp423 lacking ZF 26–30 was generated by PCR and cloned into the pMSCV vector. Retroviral production in phoenix packaging cells was achieved as previously described (Gupta et al., 2010).

ACCESSION NUMBERS

The accession number for the microarray data reported in this paper is GEO: GSE74899.

SUPPLEMENTAL INFORMATION

Supplemental Information includes Supplemental Experimental Procedures, seven figures, and two tables and can be found with this article online at http://dx.doi.org/10.1016/j.cmet.2016.04.023.

AUTHOR CONTRIBUTIONS

M.S., J.I., C.M.K., Q.A.W., C.H., L.V., K.A.M., and S.B.S. conducted the experiments; K.S. generated critical reagents; M.S., J.I., C.M.K., W.L.H., P.S., and R.K.G. designed the experiments; and M.S. and R.K.G. wrote the manuscript. All authors contributed to data analysis.

ACKNOWLEDGMENTS

The authors are grateful to members of the UTSW Touchstone Diabetes Center for useful discussions and P. Scherer and O. Gupta for critical reading of the manuscript. The authors thank the UTSW Animal Resource Center, Metabolic Phenotyping Core, Transgenic Core Facility, Pathology Core, Live Cell Imaging Core, and Microarray Core for excellent guidance and assistance with the performed experiments. This study was supported by NIDDK R03 DK099428, R01 DK104789, the Searle Scholars Program, and the American Heart Association 15BGIA22460021 to R.K.G.; the American Heart Association postdoctoral fellowship 16POST26420136 to M.S.; NIDDK K01 DK107788 to Q.A.W.; NIDDK R00 DK094973 to W.L.H.; and NIDDK 5R01DK10300802 to P.S. The graphical abstract accompanying this manuscript was designed by Visually Medical (http://www.visuallymedical.com).

Received: November 9, 2015
Revised: February 29, 2016
Accepted: April 25, 2016
Published: May 26, 2016

REFERENCES

Berry, D.C., Jiang, Y., and Graff, J.M. (2016). Mouse strains to study cold-inducible beige progenitors and beige adipocyte formation and function. Nat. Commun. *7*, 10184.

Betz, M.J., and Enerbäck, S. (2015). Human brown adipose tissue: what we have learned so far. Diabetes *64*, 2352–2360.

Cannon, B., and Nedergaard, J. (2004). Brown adipose tissue: function and physiological significance. Physiol. Rev. *84*, 277–359.

Chawla, A., Schwarz, E.J., Dimaculangan, D.D., and Lazar, M.A. (1994). Peroxisome proliferator-activated receptor (PPAR) gamma: adipose-predominant expression and induction early in adipocyte differentiation. Endocrinology *135*, 798–800.

Cohen, P., and Spiegelman, B.M. (2015). Brown and beige fat: molecular parts of a thermogenic machine. Diabetes *64*, 2346–2351.

Cypess, A.M., Weiner, L.S., Roberts-Toler, C., Franquet Elía, E., Kessler, S.H., Kahn, P.A., English, J., Chatman, K., Trauger, S.A., Doria, A., and Kolodny, G.M. (2015). Activation of human brown adipose tissue by a β3-adrenergic receptor agonist. Cell Metab. *21*, 33–38.

De Sousa, M., Porras, D.P., Perry, C.G., Seale, P., and Scimè, A. (2014). p107 is a crucial regulator for determining the adipocyte lineage fate choices of stem cells. Stem Cells *32*, 1323–1336.

Gupta, R.K., Arany, Z., Seale, P., Mepani, R.J., Ye, L., Conroe, H.M., Roby, Y.A., Kulaga, H., Reed, R.R., and Spiegelman, B.M. (2010). Transcriptional control of preadipocyte determination by Zfp423. Nature *464*, 619–623.

Gupta, R.K., Mepani, R.J., Kleiner, S., Lo, J.C., Khandekar, M.J., Cohen, P., Frontini, A., Bhowmick, D.C., Ye, L., Cinti, S., and Spiegelman, B.M. (2012). Zfp423 expression identifies committed preadipocytes and localizes to adipose endothelial and perivascular cells. Cell Metab. *15*, 230–239.

Hansen, J.B., Jørgensen, C., Petersen, R.K., Hallenborg, P., De Matteis, R., Bøye, H.A., Petrovic, N., Enerbäck, S., Nedergaard, J., Cinti, S., et al. (2004). Retinoblastoma protein functions as a molecular switch determining white versus brown adipocyte differentiation. Proc. Natl. Acad. Sci. USA *101*, 4112–4117.

Hata, A., Seoane, J., Lagna, G., Montalvo, E., Hemmati-Brivanlou, A., and Massagué, J. (2000). OAZ uses distinct DNA- and protein-binding zinc fingers in separate BMP-Smad and Olf signaling pathways. Cell *100*, 229–240.

Kajimura, S., Spiegelman, B.M., and Seale, P. (2015). Brown and beige fat: physiological roles beyond heat generation. Cell Metab. *22*, 546–559.

Kong, X., Banks, A., Liu, T., Kazak, L., Rao, R.R., Cohen, P., Wang, X., Yu, S., Lo, J.C., Tseng, Y.H., et al. (2014). IRF4 is a key thermogenic transcriptional partner of PGC-1α. Cell *158*, 69–83.

Lidell, M.E., Betz, M.J., Dahlqvist Leinhard, O., Heglind, M., Elander, L., Slawik, M., Mussack, T., Nilsson, D., Romu, T., Nuutila, P., et al. (2013). Evidence for two types of brown adipose tissue in humans. Nat. Med. *19*, 631–634.

Long, J.Z., Svensson, K.J., Tsai, L., Zeng, X., Roh, H.C., Kong, X., Rao, R.R., Lou, J., Lokurkar, I., Baur, W., et al. (2014). A smooth muscle-like origin for beige adipocytes. Cell Metab. *19*, 810–820.

Figure 7. BMP7 Signaling Disrupts the Zfp423-Ebf2 Protein Complex

(A) iWAT SVF cultures from C57BL/6 mice were co-transduced with retroviruses expressing either FLAG-tagged ZF 1–30 or mutant Zfp423 (ZF 1–25), along with full-length FLAG-Ebf2. After adipocyte differentiation, protein-protein interactions were analyzed by Ebf2 immunoblotting (anti-FLAG antibody) of Zfp423 immunoprecipitates (anti-Zfp423 antibody immunoprecipitation).

(B) iWAT SVF cells from C57BL/6 mice were transduced with retrovirus expressing FLAG-tagged Zfp423 and Ebf2 before in vitro differentiation. After differentiation, the adipocytes were treated with vehicle or browning agents (10 μM rosiglitazone, 10 μM isoproterenol, or 10 nM BMPs) for 6 hr. Protein-protein interaction was analyzed by immunoblotting of Zfp423 immunoprecipitates.

(C) iWAT SVF cells from C57BL/6 were transduced with retrovirus expressing FLAG-tagged ZF 1–30 or ΔSBD, together with retrovirus expressing Ebf2 before in vitro differentiation. After differentiation, the differentiated adipocytes were treated with vehicle or 10 nM BMP7 for 6 hr. Protein-protein interaction was analyzed by immunoblotting of Zfp423 immunoprecipitates.

(D) Proposed model for the inhibition of the thermogenic gene program in white adipocytes by Zfp423. Zfp423 binds to Ebf2 and serves as a transcriptional co-repressor at key Ebf2-target genes, such as Prdm16. This leads to a suppression of the overall thermogenic gene program in white adipocytes.

(E) Proposed model for the interaction between BMP signaling and Ebf2 signaling in brown adipocyte differentiation. BMP7 triggers a Smad1/4 interaction with Zfp423 that leads to activation of *Pparγ* expression and adipogenesis. This sequesters Zfp423 from Ebf2, thereby allowing Ebf2 to drive the thermogenic gene program of BAT.

McDonald, M.E., Li, C., Bian, H., Smith, B.D., Layne, M.D., and Farmer, S.R. (2015). Myocardin-related transcription factor A regulates conversion of progenitors to beige adipocytes. Cell *160*, 105–118.

Ohno, H., Shinoda, K., Ohyama, K., Sharp, L.Z., and Kajimura, S. (2013). EHMT1 controls brown adipose cell fate and thermogenesis through the PRDM16 complex. Nature *504*, 163–167.

Puigserver, P., Wu, Z., Park, C.W., Graves, R., Wright, M., and Spiegelman, B.M. (1998). A cold-inducible coactivator of nuclear receptors linked to adaptive thermogenesis. Cell *92*, 829–839.

Rajakumari, S., Wu, J., Ishibashi, J., Lim, H.W., Giang, A.H., Won, K.J., Reed, R.R., and Seale, P. (2013). EBF2 determines and maintains brown adipocyte identity. Cell Metab. *17*, 562–574.

Rosen, E.D., and Spiegelman, B.M. (2014). What we talk about when we talk about fat. Cell *156*, 20–44.

Sanchez-Gurmaches, J., and Guertin, D.A. (2014). Adipocytes arise from multiple lineages that are heterogeneously and dynamically distributed. Nat. Commun. *5*, 4099.

Sanchez-Gurmaches, J., Hung, C.M., and Guertin, D.A. (2016). Emerging complexities in adipocyte origins and identity. Trends Cell Biol. *26*, 313–326.

Schrauwen, P., van Marken Lichtenbelt, W.D., and Spiegelman, B.M. (2015). The future of brown adipose tissues in the treatment of type 2 diabetes. Diabetologia *58*, 1704–1707.

Seale, P. (2015). Transcriptional regulatory circuits controlling brown fat development and activation. Diabetes *64*, 2369–2375.

Seale, P., Kajimura, S., Yang, W., Chin, S., Rohas, L.M., Uldry, M., Tavernier, G., Langin, D., and Spiegelman, B.M. (2007). Transcriptional control of brown fat determination by PRDM16. Cell Metab. *6*, 38–54.

Seale, P., Bjork, B., Yang, W., Kajimura, S., Chin, S., Kuang, S., Scimè, A., Devarakonda, S., Conroe, H.M., Erdjument-Bromage, H., et al. (2008). PRDM16 controls a brown fat/skeletal muscle switch. Nature *454*, 961–967.

Seale, P., Conroe, H.M., Estall, J., Kajimura, S., Frontini, A., Ishibashi, J., Cohen, P., Cinti, S., and Spiegelman, B.M. (2011). Prdm16 determines the thermogenic program of subcutaneous white adipose tissue in mice. J. Clin. Invest. *121*, 96–105.

Sharp, L.Z., Shinoda, K., Ohno, H., Scheel, D.W., Tomoda, E., Ruiz, L., Hu, H., Wang, L., Pavlova, Z., Gilsanz, V., and Kajimura, S. (2012). Human BAT possesses molecular signatures that resemble beige/brite cells. PLoS ONE *7*, e49452.

Shinoda, K., Luijten, I.H., Hasegawa, Y., Hong, H., Sonne, S.B., Kim, M., Xue, R., Chondronikola, M., Cypess, A.M., Tseng, Y.H., et al. (2015). Genetic and functional characterization of clonally derived adult human brown adipocytes. Nat. Med. *21*, 389–394.

Sun, K., Kusminski, C.M., and Scherer, P.E. (2011). Adipose tissue remodeling and obesity. J. Clin. Invest. *121*, 2094–2101.

Tentolouris, N., Liatis, S., and Katsilambros, N. (2006). Sympathetic system activity in obesity and metabolic syndrome. Ann. N Y Acad. Sci. *1083*, 129–152.

Tontonoz, P., Hu, E., and Spiegelman, B.M. (1994). Stimulation of adipogenesis in fibroblasts by PPAR gamma 2, a lipid-activated transcription factor. Cell *79*, 1147–1156.

Townsend, K.L., An, D., Lynes, M.D., Huang, T.L., Zhang, H., Goodyear, L.J., and Tseng, Y.H. (2013). Increased mitochondrial activity in BMP7-treated brown adipocytes, due to increased CPT1- and CD36-mediated fatty acid uptake. Antioxid. Redox Signal. *19*, 243–257.

Tsai, R.Y., and Reed, R.R. (1997). Cloning and functional characterization of Roaz, a zinc finger protein that interacts with O/E-1 to regulate gene expression: implications for olfactory neuronal development. J. Neurosci. *17*, 4159–4169.

Tsai, R.Y., and Reed, R.R. (1998). Identification of DNA recognition sequences and protein interaction domains of the multiple-Zn-finger protein Roaz. Mol. Cell. Biol. *18*, 6447–6456.

Tseng, Y.H., Kokkotou, E., Schulz, T.J., Huang, T.L., Winnay, J.N., Taniguchi, C.M., Tran, T.T., Suzuki, R., Espinoza, D.O., Yamamoto, Y., et al. (2008). New role of bone morphogenetic protein 7 in brown adipogenesis and energy expenditure. Nature *454*, 1000–1004.

Villanueva, C.J., Waki, H., Godio, C., Nielsen, R., Chou, W.L., Vargas, L., Wroblewski, K., Schmedt, C., Chao, L.C., Boyadjian, R., et al. (2011). TLE3 is a dual-function transcriptional coregulator of adipogenesis. Cell Metab. *13*, 413–427.

Villanueva, C.J., Vergnes, L., Wang, J., Drew, B.G., Hong, C., Tu, Y., Hu, Y., Peng, X., Xu, F., Saez, E., et al. (2013). Adipose subtype-selective recruitment of TLE3 or Prdm16 by PPARγ specifies lipid storage versus thermogenic gene programs. Cell Metab. *17*, 423–435.

Virtanen, K.A., Lidell, M.E., Orava, J., Heglind, M., Westergren, R., Niemi, T., Taittonen, M., Laine, J., Savisto, N.J., Enerbäck, S., and Nuutila, P. (2009). Functional brown adipose tissue in healthy adults. N. Engl. J. Med. *360*, 1518–1525.

Vishvanath, L., MacPherson, K.A., Hepler, C., Wang, Q.A., Shao, M., Spurgin, S.B., Wang, M.Y., Kusminski, C.M., Morley, T.S., and Gupta, R.K. (2016). Pdgfrβ(+) mural preadipocytes contribute to adipocyte hyperplasia induced by high-fat-diet feeding and prolonged cold exposure in adult mice. Cell Metab. *23*, 350–359.

Wang, Q.A., Tao, C., Gupta, R.K., and Scherer, P.E. (2013). Tracking adipogenesis during white adipose tissue development, expansion and regeneration. Nat. Med. *19*, 1338–1344.

Wang, W., Kissig, M., Rajakumari, S., Huang, L., Lim, H.W., Won, K.J., and Seale, P. (2014). Ebf2 is a selective marker of brown and beige adipogenic precursor cells. Proc. Natl. Acad. Sci. USA *111*, 14466–14471.

Warming, S., Rachel, R.A., Jenkins, N.A., and Copeland, N.G. (2006). Zfp423 is required for normal cerebellar development. Mol. Cell. Biol. *26*, 6913–6922.

Zhang, H., Schulz, T.J., Espinoza, D.O., Huang, T.L., Emanuelli, B., Kristiansen, K., and Tseng, Y.H. (2010). Cross talk between insulin and bone morphogenetic protein signaling systems in brown adipogenesis. Mol. Cell. Biol. *30*, 4224–4233.

Cell Metabolism, Volume *23*

Supplemental Information

Zfp423 Maintains White Adipocyte Identity through Suppression of the Beige Cell Thermogenic Gene Program

Mengle Shao, Jeff Ishibashi, Christine M. Kusminski, Qiong A. Wang, Chelsea Hepler, Lavanya Vishvanath, Karen A. MacPherson, Stephen B. Spurgin, Kai Sun, William L. Holland, Patrick Seale, and Rana K. Gupta

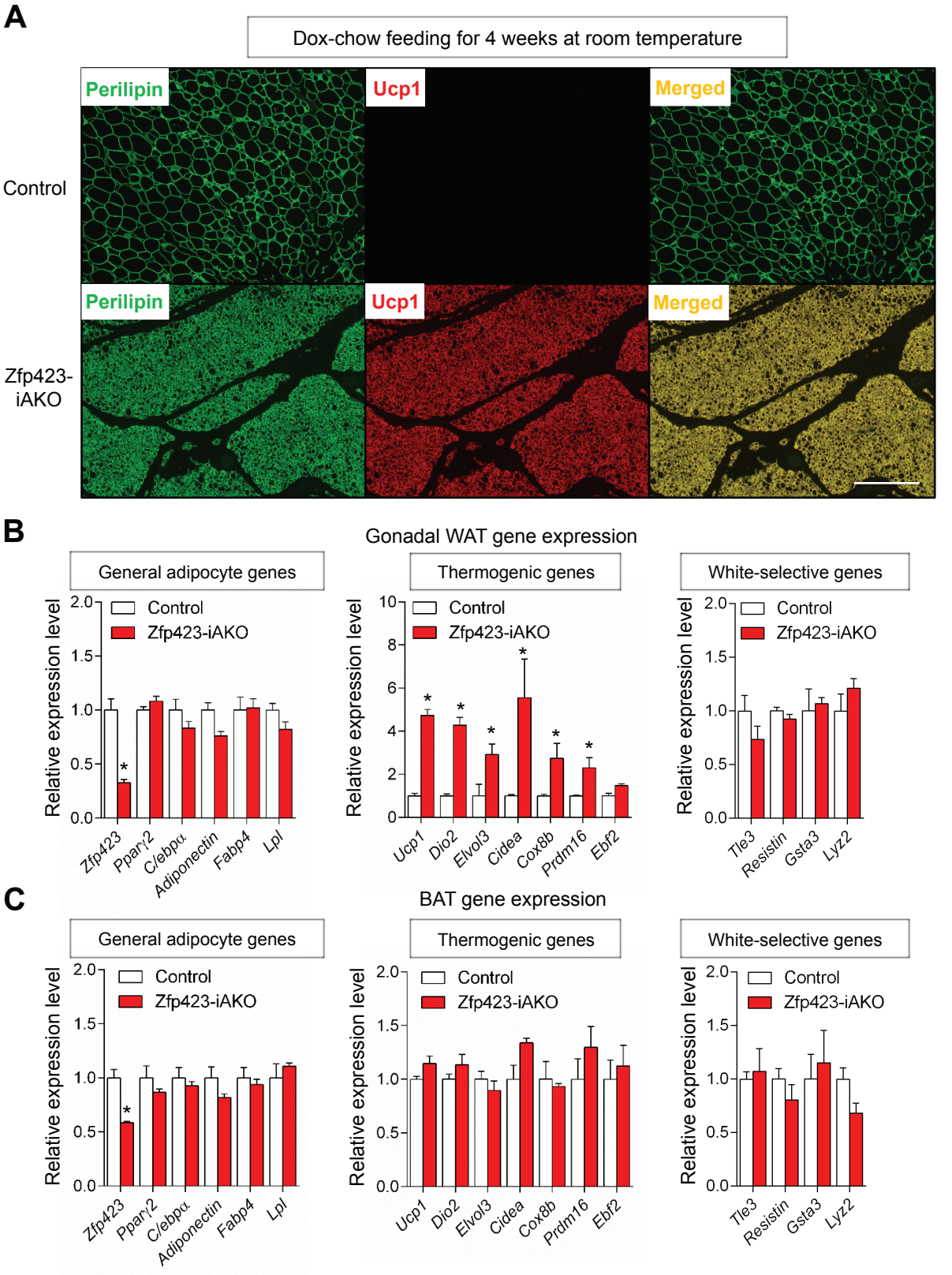

Figure S1: Related to Figure 1

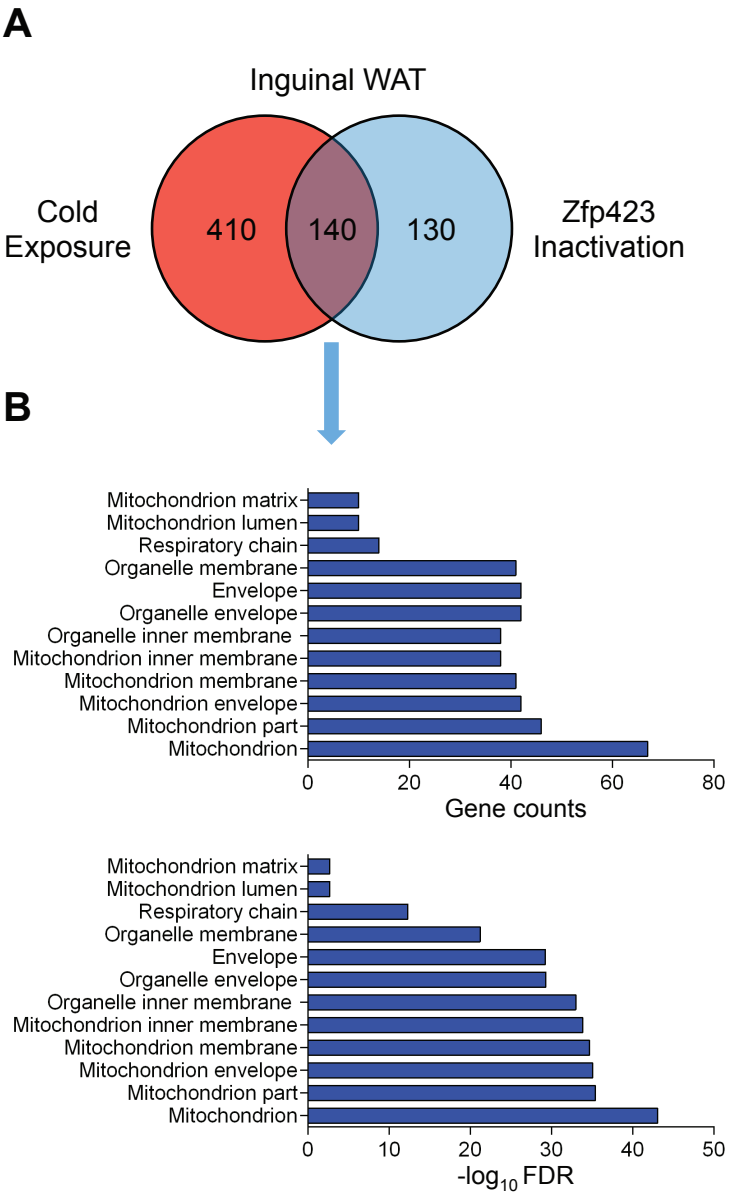

Figure S2: Related to Figure 1

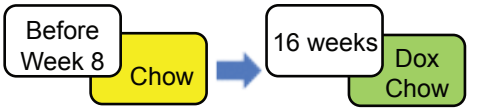

Dox feeding for 16 weeks at room temperature

Inguinal WAT

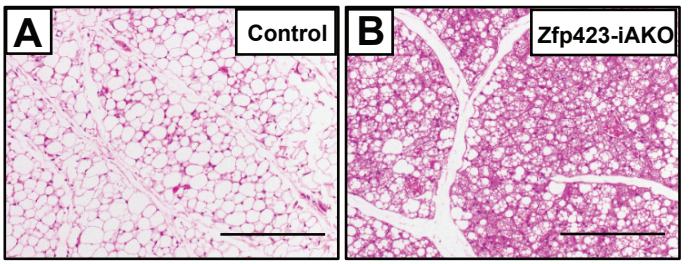

C

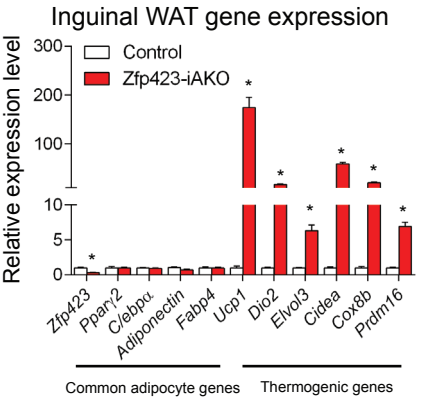

Perirenal WAT

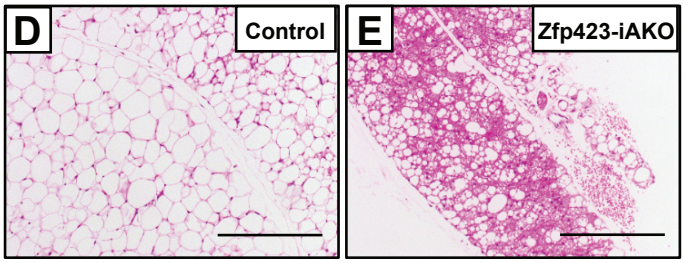

F

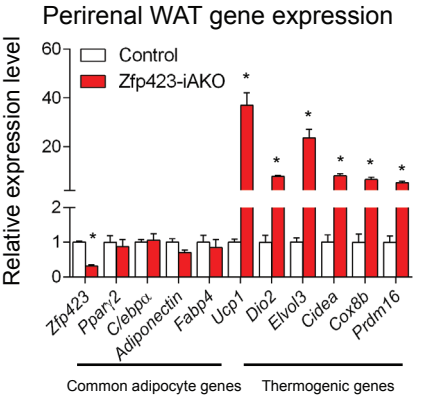

Gonadal WAT

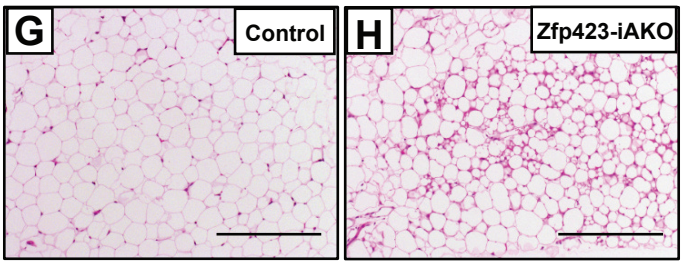

I

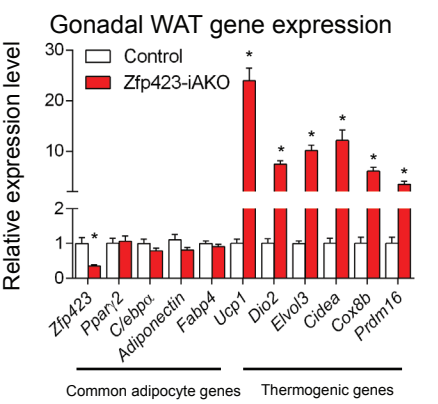

Figure S3: Related to Figure 1

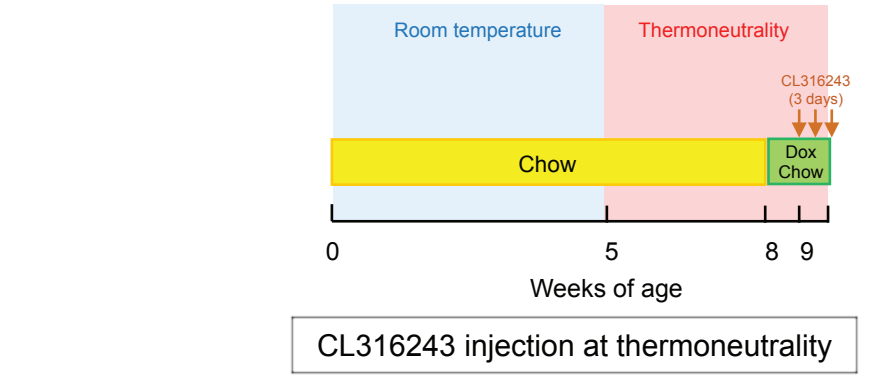

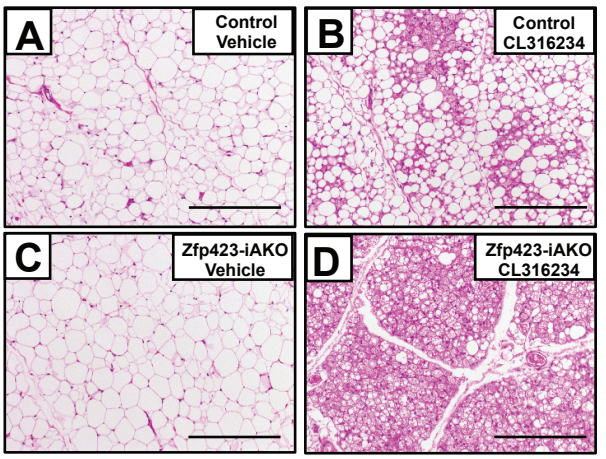

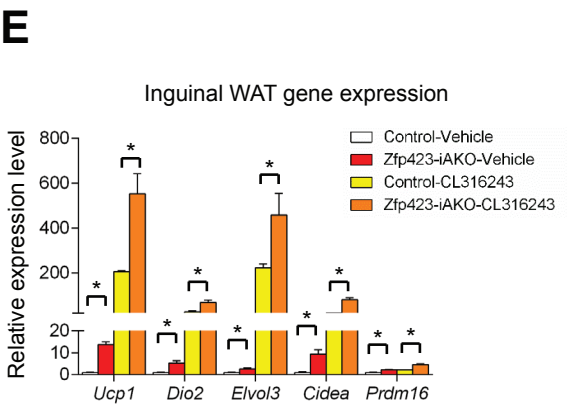

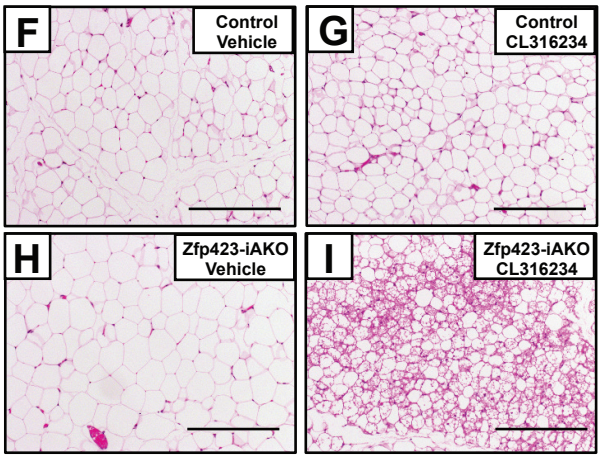

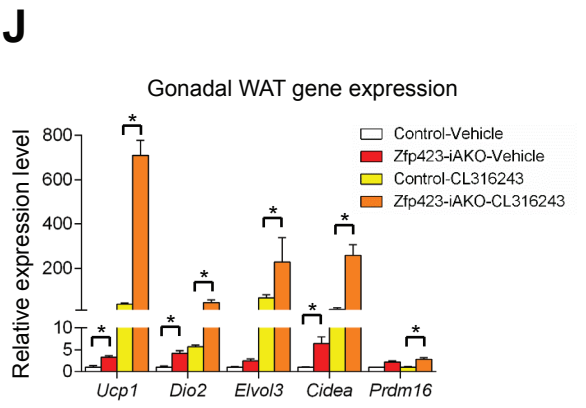

Figure S4: Related to Figure 1

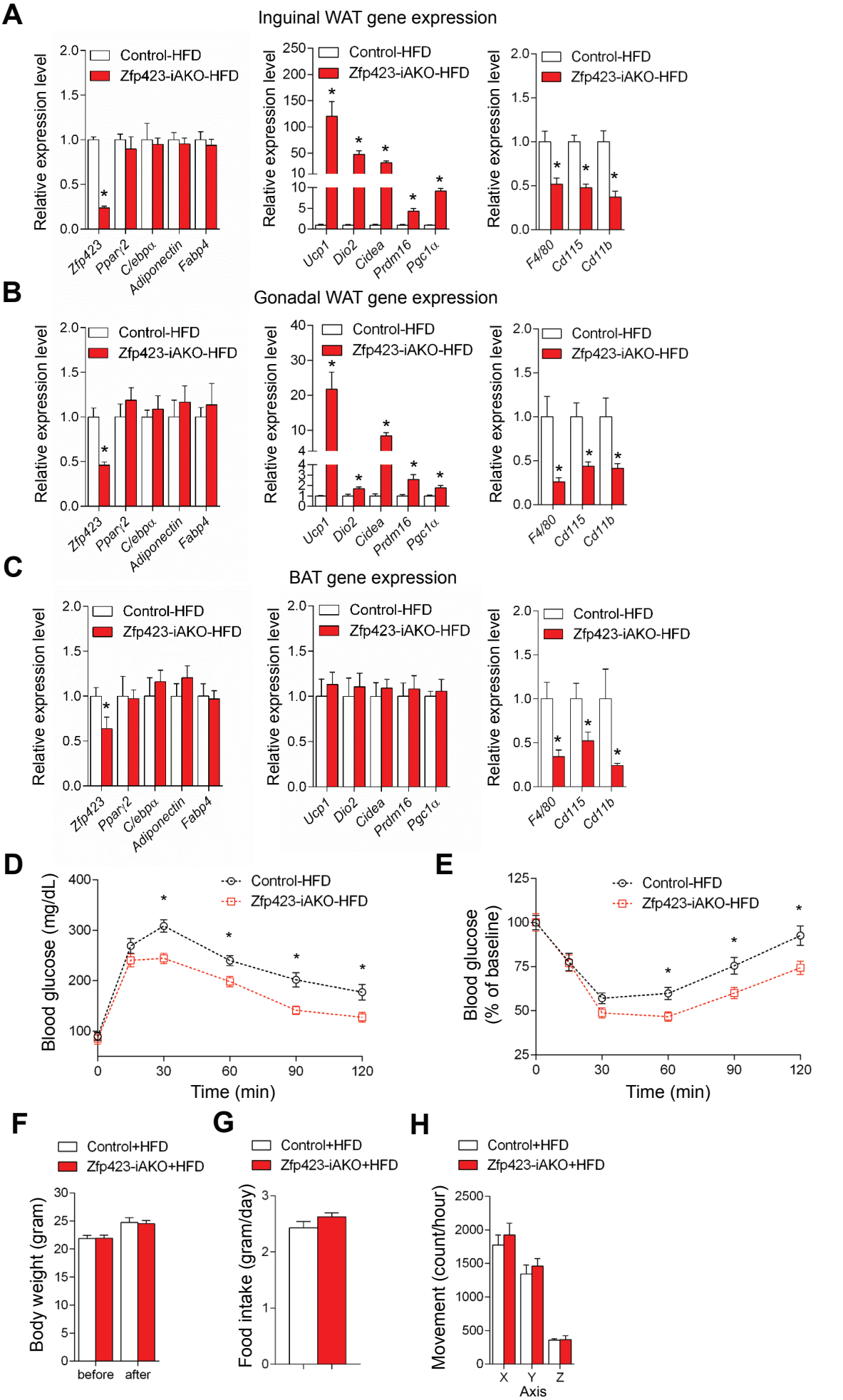

Figure S5: Related to Figure 3

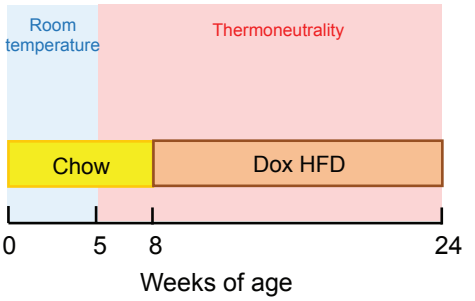

A

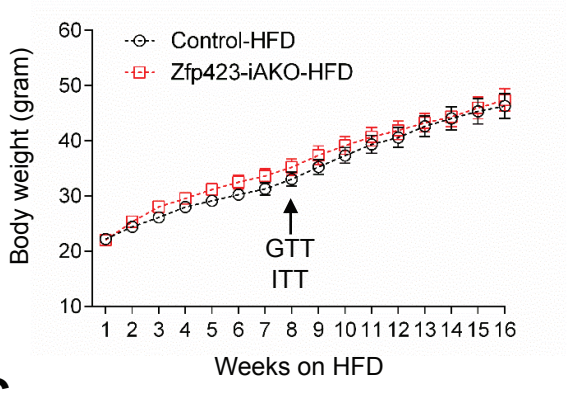

B

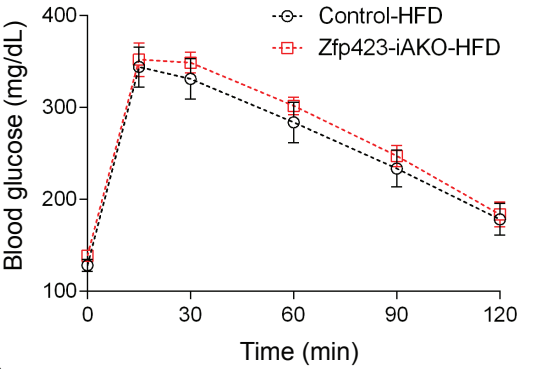

C

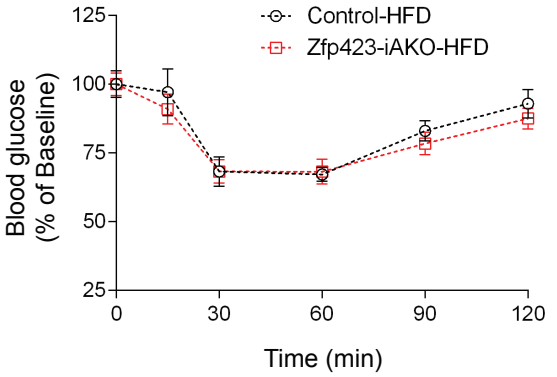

D

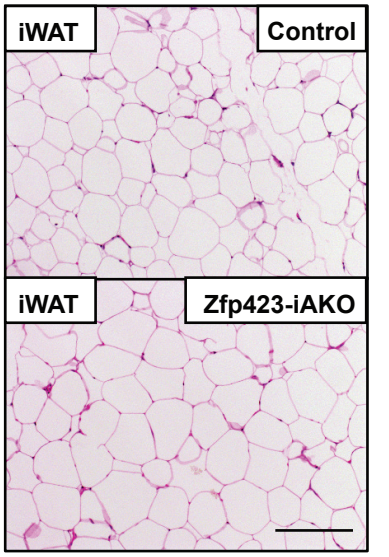

Figure S6: Related to Figure 3

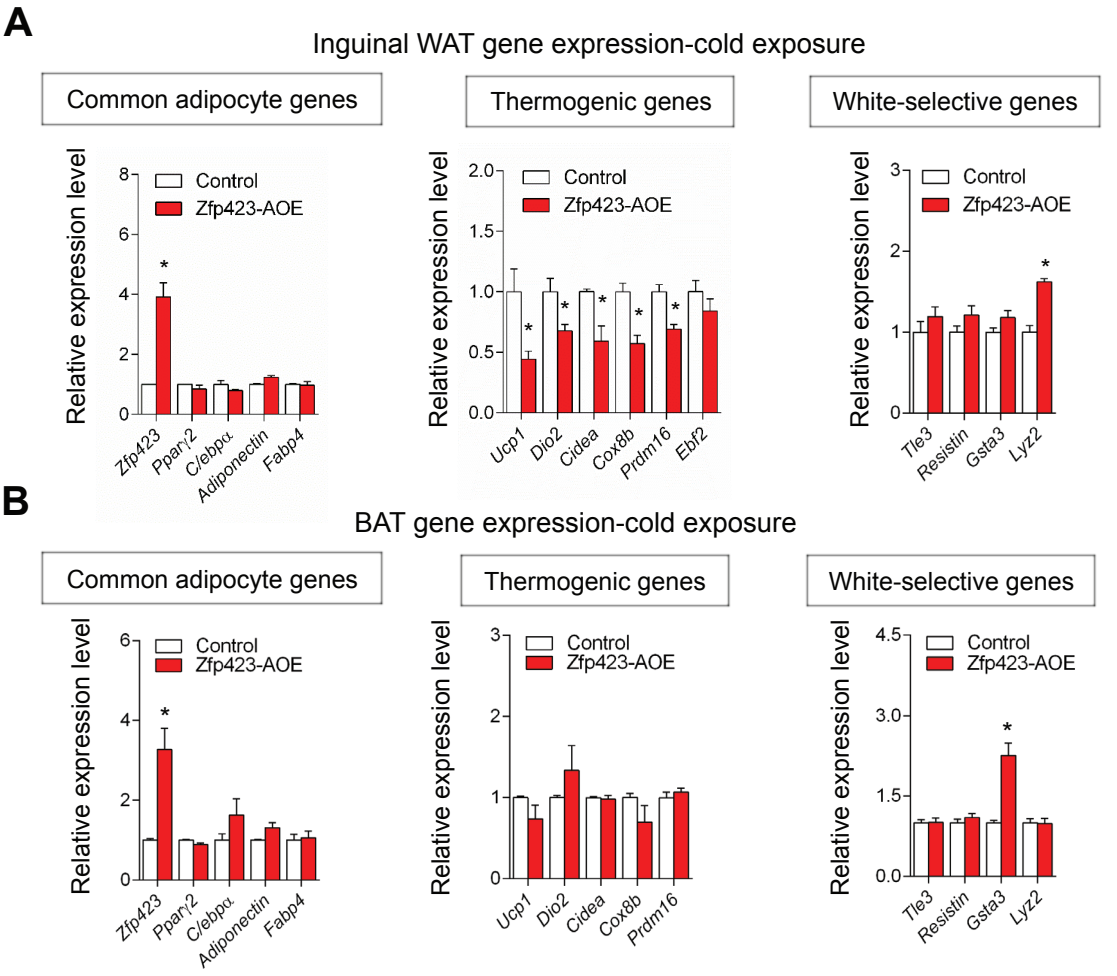

Figure S7: Related to Figure 5

Supplemental Figure Legends

Figure S1. Related to Figure 1

(A) Indirect Immunofluorescence staining of Perilipin (green) and Ucp1 (red) in iWAT paraffin sections prepared from control and Zfp423-iAKO mice after dox feeding.

(B) Relative mRNA levels of common adipocyte genes, thermogenic genes, and white adipocyte-selective genes in the gonadal white adipose tissue (gWAT) of control and Zfp423-iAKO mice after dox feeding. * denotes $p<0.05$ from Student's t-test. n=4.

(C) Relative mRNA levels of common adipocyte genes, thermogenic genes, and white adipocyte-selective genes in the interscapular brown adipose tissue (BAT) of control and Zfp423-iAKO mice after dox feeding. * denotes $p<0.05$ from Student's t-test. n=4.

Figure S2. Related to Figure 1

(A) Global gene expression profiles (microarray analysis) were obtained using total RNA extracted from iWAT of:

Cohort 1: Control mice maintained at room temperature on dox-containing chow diet for 28 days.
Cohort 2: Age-matched Zfp423-iAKO mice maintained at room temperature on dox-containing chow diet for 28 days.
Cohort 3: Control mice maintained on dox-containing chow diet for 28 days, with the last 14 days at 6°C to induce the formation of beige adipocytes.

Venn diagram depicting overlap between genes whose expression is significantly altered (fold change >2.0 and ANOVA p-value < 0.05) by cold exposure (Cohort 1 vs. 3) or Zfp423 inactivation (Cohort 1 vs. 2).

(B) Gene ontology analysis of the 140 genes commonly altered by cold exposure or Zfp423 inactivation.

Figure S3. Related to Figure 1

(A,B) Control and Zfp423-iAKO mice were housed at room temperature and fed on normal chow until 8 weeks of age before switching to doxycycline (dox)-containing chow diet for another 16 weeks. Representative H&E staining of the inguinal WAT from control and Zfp423-iAKO mice after 16 weeks dox feeding. Scale bar=200μM.

(C) Relative mRNA levels of common adipocyte genes and thermogenic genes in inguinal WAT from control and Zfp423-iAKO mice after 16 weeks dox feeding. * denotes $p<0.05$ from Student's t-test. n=6.

(D,E) Representative H&E staining of the perirenal WAT from control and Zfp423-iAKO mice after 16 weeks dox feeding. Scale bar=200μM.

(F) Relative mRNA levels of common adipocyte genes and thermogenic genes in perirenal WAT from control and Zfp423-iAKO mice after 16 weeks dox feeding. * denotes $p<0.05$ from Student's t-test. n=6.

(G,H) Representative H&E staining of the gonadal WAT from control and Zfp423-iAKO mice after 16 weeks dox feeding. Scale bar=200μM.

(I) Relative mRNA levels of common adipocyte genes and thermogenic genes in gonadal WAT from control and Zfp423-iAKO mice after 16 weeks of dox feeding. * denotes $p<0.05$ from Student's t-test. n=6.

Figure S4. Related to Figure 1

(A-D) Control and Zfp423-iAKO mice were housed at room temperature until 5 weeks of age before switching to thermoneutral housing. Mice were fed on normal chow until 8 weeks of age before switching to doxycycline (dox)-containing chow diet. After 1 week of dox feeding, mice were intraperitoneally injected with vehicle or CL316243 (1mg/kg/day) for 3 days. Representative H&E staining of the inguinal WAT from control and Zfp423-iAKO mice after vehicle or CL316243 injection. Scale bar=200μM.

(E) Relative mRNA levels of indicated genes in inguinal WAT from control and Zfp423-iAKO mice after vehicle or CL316243 injection. * denotes $p<0.05$ from two-way ANOVA. n=4.

(F-I) Representative H&E staining of the gonadal WAT from control and Zfp423-iAKO mice after vehicle or CL316243 injection. Scale bar=200μM.

(J) Relative mRNA levels of indicated genes in gonadal WAT from control and Zfp423-iAKO mice after vehicle or CL316243 injection. * denotes $p<0.05$ from two-way ANOVA. n=4.

Figure S5. Related to Figure 3

(A-C) Relative mRNA levels of indicated genes in iWAT (A), gWAT (B) and BAT (C) of control and Zfp423-iAKO mice after 16 weeks of dox-HFD feeding. * denotes $p<0.05$ from Student's t-test. n=6.

(D-E) Glucose tolerance test (GTT) and insulin tolerance test (ITT) of control and Zfp423-iAKO after 8 weeks of dox-HFD feeding. * denotes $p<0.05$ from Student's t-test. n=6-8.

(F) Body weight of control and Zfp423-iAKO mice before and after the metabolic cage measurements after 3 weeks of dox-HFD feeding. n=6.

(G) Daily food intake of control and Zfp423-iAKO mice during the 5-day metabolic cage measurements after 3 weeks of dox-HFD feeding. n=6.

(H) Physical activity of control and Zfp423-iAKO mice during the 5-day metabolic cage measurements after 3 weeks of dox-HFD feeding. n=6.

Figure S6. Related to Figure 3

(A) Control and Zfp423-iAKO mice were housed at room temperature until 5 weeks of age before switching to a thermoneutral environment. Mice were fed a standard chow diet until 8 weeks of age before switching to dox-containing high fat diet (HFD) at thermoneutrality. Body weights of control and Zfp423-iAKO mice were measured weekly. n=7-8.

(B, C) Glucose tolerance test **(B)** and insulin tolerance test **(C)** of control and Zfp423-iAKO mice after 8 weeks of dox-HFD feeding at thermoneutrality. n=7-8.

(D) Representative H&E staining of inguinal WAT of control and Zfp423-iAKO mice after 16 weeks of dox-HFD feeding at thermoneutrality. Scale bar=200μM.

Figure S7. Related to Figure 5

(A) Relative mRNA levels of common adipocyte genes, thermogenic genes, and white adipocyte-selective genes in iWAT of cold-exposed (7 days), dox-fed, control and Zfp423-AOE mice. * denotes $p<0.05$ from Student's t-test. n=4.

(B) Relative mRNA levels of common adipocyte genes, thermogenic genes, and white adipocyte-selective genes in BAT of cold-exposed (7 days), dox-fed, control and Zfp423-AOE mice. * denotes $p<0.05$ from Student's t-test. n=4.

Supplemental Tables

Table 1: Related to Figure 1
Genes differentially regulated in inguinal WAT of Zfp423-iAKO mice

Table 2: Related to Experimental Procedures
qPCR primer sequences used in this study

Gene	Forward 5'-3'	Reverse 5'-3'
Zfp423	CAGGCCCACAAGAAGAACAAG	GTATCCTCGCAGTAGTCGCACA
Pparγ2	GCATGGTGCCTTCGCTGA	TGGCATCTCTGTGTCAACCATG
C/ebpα	TGGCCTGGAGACGCAATGA	CGCAGAGATTGTGCGTCTTT
Adiponectin	AGATGGCACTCCTGGAGAGAA	TTCTCCAGGCTCTCCTTTCCT
Fabp4	GATGAAATCACCGCAGACGAC	ATTCCACCACCAGCTTGTCAC
Lpl	CATCGAGAGAGGATCCGAGTGAA	TGCTGAGTCCTTTCCCTTCTG
Ucp1	TCTCAGCCGGCTTAATGACTG	GGCTTGCATTCTGACCTTCAC
Dio2	CATTGATGAGGCTCACCCTTC	GGTTCCGGTGCTTCTTAACCT
Elvol3	GTGTGCTTTGCCATCTACACG	CTCCCAGTTCAACAACCTTGC
Cidea	TCCTATGCTGCACAGATGACG	TGCTCTTCTGTATCGCCCAGT
Cox8b	TGCTGGAACCATGAAGCCAAC	AGCCAGCCAAAACTCCCACTT
Prdm16	ACACGCCAGTTCTCCAACCTGT	TGCTTGTTGAGGGAGGAGGTA
Ebf2	GCTGCGGGAACCGGAACGAGA	ACACGACCTGGAACCGCCTCA
Tle3	GAGACTGAACACAATCCTAGCC	GGAGTCCACGTACCCCGAT
Resistin	AAGAACCTTTCATTTCCCCTCCT	GTCCAGCAATTTAAGCCAATGTT
Gsta3	AGATCGACGGGATGAAACTGG	CAGATCCGCCACTCCTTCT
Lyz2	GAATGGAATGGCTGGCTACT	CGTGCTGAGCTAAACACACC
Cited1	AACCTTGGAGTGAAGGATCGC	GTAGGAGAGCCTATTGGAGATGT
Ear2	CCACAAAGCAGACAGGGAAAC	GCATGAGGCAAGCATTAGGAC
Tmem26	AGGGGCTTCCTTAGGGTTTTC	CCGTCTTGGATGAAGAAGCTG

Hoxa9	CCCCGACTTCAGTCCTTGC	GATGCACGTAGGGGTGGTG
Lhx8	GAGCTCGGACCAGCTTCA	TTGTTGTCCTGAGCGAACTG
Zic1	CTGTTGTGGGAGACACGATG	CCTCTTCTCAGGGCTCACAG
Pgc1α	GCACCAGAAAACAGCTCCAAG	CGTCAAACACAGCTTGACAGC
F4/80	TGACTCACCTTGTGGTCCTAA	CTTCCCAGAATCCAGTCTTTCC
Cd115	TGTCATCGAGCCTAGTGGC	CGGGAGATTCAGGGTCCAAG
Cd11b	GGCTCCGGTAGCATCAACAA	ATCTTGGGCTAGGGTTTCTCT
Rps18	CATGCAAACCCACGACAGTA	CCTCACGCAGCTTGTTGTCTA

Supplemental Experimental Procedures

Rodent Diets and Drug treatments. Mice were maintained on standard rodent chow or similar chow containing 600 mg/kg doxycycline (dox) (Bio-Serv, S4107). For high-fat diet studies, mice were fed a standard high-fat diet (60 kcal% fat, Research Diets, D12492i) or doxycycline-containing high fat diet (600 mg/kg dox, 60% kcal% fat, Bio-Serv, S5867) as described in the text. For chronic β-3 adrenergic agonist administration, mice were anesthetized by 2% isoflurane and Alzet osmotic minipumps filled with vehicle (PBS) or CL 316423 (1mg/kg/24hr) were implanted subcutaneously in the mid-back region.

Derivation of TRE-Zfp423 mice. To generate a doxycycline-inducible mouse model of *Zfp423* overexpression (TRE-Zfp423), full-length cDNA encoding mouse *Zfp423* was subcloned into the pTRE vector (Clontech) with the restriction sites HindIII and BamHI. To better stabilize the transcript and enhance translation, a Kozak sequence 5'-GCCGCCACC-3' was inserted in front of the start codon and the rabbit β-globin 3' untranslated region (UTR) was cloned into the 3' end of the vector. After linearization (SalI digestion) and purification, TRE-Zfp423 DNA was injected into embryos of a pure C57BL/6 background by the Transgenic Core Facility at UT Southwestern Medical Center. Founders and offspring were identified by SYBR green qPCR using the following primers (5' to 3'):
TreZfp423F: CAGAGTTGCAGAACCACACGA
TreZfp423R: atcaagggtccccaaactcac

Metabolic analysis. Metabolic cage studies were conducted using a Comprehensive Lab Animal Monitoring System (CLAMS, Columbus Instruments) at USTW Metabolic Phenotyping Core. Mice were acclimated in the metabolic chambers for 5 days before the start of the experiments. Food intake, movement, and CO_2 and O_2 levels were measured every 60 min for each mouse over a period of 5 days. For glucose tolerance tests (GTT), mice were injected i.p. with glucose (Sigma) at the dosage of 1g per kg body weight after an overnight fast. For insulin tolerance test, mice were injected i.p. with 0.75 U human insulin (Eli Lilly) per kg body weight after a fast of 6 hours. Blood was collected by venous bleeding from the tail vein at 0, 15, 30, 60, 90 and 120 min post injection. Glucose concentrations were measured using Bayer Contour glucometers.

Mitochondrial function and respiration. Mitochondrial oxygen consumption rates (OCRs) from minced adipose depots were determined using a XF24 Extracellular Flux Analyzer (Seahorse Bioscience, MA). A basal-oligomycin- carbonyl cyanide 4-(trifluoromethoxy)phenylhydrazone (FCCP)-antimycin-A/rotenone "BOFA" experiment was utilized for the *ex vivo* assessment of mitochondrial function and respiration rates in whole adipose tissues. In brief, whole adipose tissue slices (~20 mg) were locked into an XF24 islet-capture Microplate (Seahorse Bioscience). Tissues were then equilibrated for 1 h at 37^{o}C (non-CO_2) in XF Assay Medium (Modified DMEM, 0 mM Glucose; Seahorse Bioscience) (pH 7.4), supplemented with 1mM sodium pyruvate, 1 mM L-

Glutamine and 7 mM glucose. The XF24 plate was then transferred to a temperature-controlled (37 °C) Seahorse analyzer and subjected to a 10-min equilibration period and 3 assay cycles to measure the basal rate, comprising a 3-min mix, a 2-min wait and a 3-min measure period each. Compounds were then added by automatic pneumatic injection followed by assay cycles after each, comprising of 3-min mix, 2-min wait and a 3-min measure period. OCR measurements were obtained following sequential additions of oligomyin (1 μM final concentration), FCCP (1 μM) and antimycin-A/rotenone (10 μM/100 nM). OCR measurements were recorded at set interval time-points. All compounds and materials above were obtained from Sigma-Aldrich.

Isolation of WAT and BAT stromal vascular cells. White fat tissues dissected from mice (4-5 weeks of age) were washed in PBS, minced thoroughly, and digested in vacuum filtered digestion buffer (100mM Hepes PH 7.4, 120 mM NaCl, 50 mM KCl, 5 mM glucose, 1 mM CaCl2, 1.5% bovine serum albumin, and 1mg ml^{-1} collagenase D) for 2 hours at 37°C with shaking. Digested tissues were then filtered through 100 μM cell strainers to remove undigested tissues. The flow-through was centrifuged for 5 min at 600 g to pellet the stromal vascular cells. The floating adipocyte layer was discarded and the stromal vascular cells were re-suspended in growth media as described in the Experimental Procedures. Brown fat tissues dissected from mice (7-14 days of age) were washed in PBS, minced thoroughly, and digested in vacuum filtered digestion buffer (50 mM Hepes PH 7.4, 62 mM NaCl, 2.5 mM KCl, 2.5 mM glucose, 0.65 mM CaCl2, 2% bovine serum albumin, and 0.75 mg ml^{-1} collagenase B) for 45 min at 37°C with shaking. Digested tissues were then filtered through 100 μM cell strainers to remove undigested tissues. The flow-through was centrifuged for 5 min at 600 g to pellet the stromal vascular cells. The floating adipocyte layers was removed and the stromal vascular cells were re-suspended in growth media as described in the Experimental Procedures. For cell sorting by flow cytometry, isolated SVF cells were labelled with indicated antibodies and cell sorting was conducted at UT Southwestern Medical Center Flow Cytometry Core Facility as previously described(Vishvanath et al., 2016).

Oil red O staining. Differentiated cells were fixed in 10% formalin for 10 min at room temperature. Following fixation, the cells were washed with deionized water twice and incubated in 60% isopropanol for 5 min. Then the cells were completely air dried at room temperature before Oil red O working solution (2 g l^{-1} Oil red O in 60% isopropanol) was added. After incubation at room temperature for 10 min, the Oil red O solution was removed and the cells were washed with deionized water for 4 times before the images were acquired for analysis.

Lentiviral CRISPR and lentivirus production. Lentiviral CRISPR plasmid targeting Ebf2 was constructed by cloning Ebf2 gRNA sequence 5' GTGCCGAGATGGATTCGGTC 3' into the LentiCRISPR (v1) plasmid backbone (Addgene plasmid # 49535). For lentivirus production, 10 μg lentiviral CRISPR constructs were transfected using Lipofectamine LTX (Invitrogen) into Phoenix packaging cells along with 5 μg pCMV-VSV-G (Addgene # 8454) and 5 μg psPAX2 (Addgene # 12260). Viral supernatants were harvested 48 hours after transfection. For viral infection, viral supernatants were added to the stromal vascular cells for 24 hours

in the presence of polybrene (8 μg/ml). Cells were then allowed to grow to confluence for *in vitro* differentiation.

Co-immunoprecipitation assays. Cells were lysed in Pierce IP lysis buffer (Thermo Scientific) supplemented with 1% Protease Inhibitor Cocktail (Sigma). After incubation with the indicated antibodies at 4°C overnight, immune complexes were captured by mixing with protein G-Sephrose beads (GE Healthcare Bio-sciences) for 1 hour at room temperature. After washing with Pierce IP lysis buffer for 3 times, samples were eluted by boiling in 2 X SDS loading buffer and resolved by SDS-polyacrylamide gel electrophoresis (SDS-PAGE) and immunoblotting.

Immunoblotting and antibodies. Protein extracts from cells or tissues were prepared by homogenization in RIPA lysis buffer (Santa Cruz). Protein extracts were separated by SDS-polyacrylamide gel electrophoresis (SDS-PAGE) and transferred onto PVDF membrane (Millipore). After incubation with the indicated primary antibodies at 4°C overnight, the blots were incubated with IR Dye- coupled secondary antibodies (LI-COR) and visualized by the LI-COR Odyssey infrared imaging system. The anti-Zfp423 antibody for immunoprecipitation was purchased from Santa Cruz Biotechnology (sc-48785), the anti-Zfp423 antibody for immuoblotting was from BD Biosciences (R94920). The anti-Ucp1 antibody was purchased from Abcam (ab10983), the anti-Ebf2 antibody was from R&D systems (AF7006), the anti-FLAG (F1804) and anti-β-actin (A1978) antibodies were from Sigma, and the anti-Smad 1 (#6944) and anti-Smad 5 (#9515) antibodies were from Cell Signaling.

Indirect Immunofluorescence. The following antibodies and concentrations were used: guinea pig anti-perilipin 1:1500 (Fitzgerald 20R-PP004); rabbit anti-UCP1 1:500 (Abcam, ab10983); rabbit anti-GFP 1:700 (Abcam, ab13970); donkey anti-rabbit Alexa 647 1:200 (Invitrogen); and goat anti-guinea pig Alexa 488 1:200 (Invitrogen). Paraffin sections were dewaxed and hydrated in Xylene and 100%-95%-80%-70%-50% Ethanol and ddH_2O. Slides were placed in chambers containing 1% R-Buffer Buffer A pH 6.0 solution and antigen retrieval was done using Antigen Retriever 2100 (Electron Microscopy Sciences) for 2 hours. Following PBS wash for 5 minutes, Fx Signal Enhancer (Invitrogen) was added to the slides for 30 minutes at room temperature. Slides were then blocked for 30 minutes in PBS containing 10% normal goat serum at room temperature. Primary antibodies were then diluted in PBS containing 10% normal goat serum and added to paraffin sections overnight at 4°C. Following washes in PBS, slides were then incubated with secondary antibodies diluted in PBS containing 10% normal goat serum for 2 hours at room temperature. Washed slides were then mounted with Prolong Anti-Fade mounting medium containing DAPI (Invitrogen). For GFP immunostaining, animals were perfused using 4% PFA before dissection.

Luciferase Gene Reporter Assays. For luciferase assays, NIH3T3 cells (125,000/well) were transfected overnight in 24-well plates using Lipofectamine 2000 (Thermo Fisher Scientific) with 600-700 ng luciferase reporter (pGL4-Prdm16(25k) (Rajakumari et al., 2013), 0.1 ng Renilla reporter (pRL-CMV), and 300-400 ng of appropriate expression plasmids (pcDNA3-Flag-Zfp423, pcDNA3-Flag-Ebf2, pcDNA3-Pparγ2, pSport-RXRα) or empty vectors (pcDNA3.1, pSport). Cells were harvested ~48 hours after transfection into 100 μl of passive lysis buffer (Promega). Luciferase activity was measured using

the dual luciferase assay kit (Promega) and a Synergy HT or H1 plate reader (Biotek). Renilla activity was used for internal normalization (Firefly/Renilla ratio) and data is presented as mean + SEM (n=3) relative to empty-vector control.

Supplemental References

Rajakumari, S., Wu, J., Ishibashi, J., Lim, H.W., Giang, A.H., Won, K.J., Reed, R.R., and Seale, P. (2013). EBF2 determines and maintains brown adipocyte identity. Cell Metab *17*, 562-574.

Vishvanath, L., MacPherson, K.A., Hepler, C., Wang, Q.A., Shao, M., Spurgin, S.B., Wang, M.Y., Kusminski, C.M., Morley, T.S., and Gupta, R.K. (2016). Pdgfrbeta(+) Mural Preadipocytes Contribute to Adipocyte Hyperplasia Induced by High-Fat-Diet Feeding and Prolonged Cold Exposure in Adult Mice. Cell Metab *23*, 350-359.